

Regulation of Actin Polymerization by JMY:
Nucleation of Filaments and Activation of the Arp2/3 Complex
to Control Cell Motility

by

J. Bradley Zuchero

DISSERTATION

Submitted in partial satisfaction of the requirements for the degree of

DOCTOR OF PHILOSOPHY

in

Biochemistry

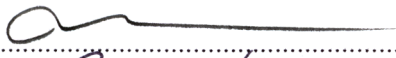


in the

GRADUATE DIVISION

of the

UNIVERSITY OF CALIFORNIA, SAN FRANCISCO

Approved:


.....

.....

.....
.....
Committee in Charge

Acknowledgements

I would like to thank the many people who made this work possible, as well as incredibly rewarding and enjoyable:

My thesis committee, Ron Vale and Wallace Marshall. Ron is my scientific and professional role model. Thank you for all of your mentoring and good will, and for including me in your miniature lab-in-exile in Woods Hole. Wallace, I thank for your enthusiasm, your creativity, and your fervent head nods to let me know when I am on the right track. I hope to continue learning from the both of you in the years to come.

Orion Weiner, the unofficial fourth member of my committee. Orion has generously given up his time to share expertise, reagents, and even his own blood with me. He has gone above and beyond what I would ever expect from a professor who is not my own direct mentor, and I am deeply indebted to him for all he has done for me. Members of his lab, especially Sarah Wilson for invaluable help with HL-60 cell culture. Henry Bourne, for stressing the importance of the Big Picture, and helping to convey that in writing.

Alex Kelly, for putting me on the right track with a simple idea and a tube of JMY plasmid DNA. Orkun Akin: Mentor. Trailblazer. Patriot. And a great friend. I have learned more from you than probably any other single person, and I am forever indebted to you. Margot Quinlan, another incredible scientist, mentor and friend. Chris Campbell, dear friend and skeptic. May your “luck” be always what you make it, and may everything you touch be golden. Scott Hansen and Lauren Goins, meticulous scientists and wonderful humans. Phoebe Grigg, for making

everything run smoothly, and helping us pin down our boss. Roberto Albanese, for taking care of his adopted lab families with meticulous work and good humor. Julianne Richter, for ensuring that all of the equipment I used in my first 5 years worked without fail. All the other members of the Mullins Lab, past and present. Your collegiality and camaraderie have made the experience one of great pleasure. I have learned so much from you, of life and science, and regard you as my extended family. Members of the Vale lab, who contributed to my growth as a scientist nearly as much as the Mullins lab. Thank you all for your time, patience, suggestions, reagents, and good will.

Rotation students who contributed to the early work on JMY: Paul Temkin for his humor and long hours at the fluorimeter, and Eugene Oh for his efforts to clone GFP-JMY. Wood Hole Physiology students, who enriched my life in countless ways, not the least of which was to reinvigorate me with my science: Team JMY 2007, Christina Vizcarra and Shang Cai; Team JMY 2008, H. Hewitt Tuson, P. Myron Miller, and D. Shane Courson; Team Nuclear Actin 2008, Daphne Manoussaki and Dave Van Valen. And of course the Cell Division Group 2009, Ron, Sarah Goodwin and Sabine Petry.

Mike D'Ambrosio, for his time and expertise setting up the IX Micro automated microscope, to save me a little slice of sanity. Carol Peebles, for fun conversations and culturing primary neurons. Andrew Carter, for useful Matlab scripts. Eric Griffis and Thomas Huckaba for plasmids, advice, and much help with cell culture. Ken Campellone and Matt Welch for their extreme collegiality;

they independently discovered JMY as a putative Arp2/3 activator but focused entirely on WHAMM in their beautiful Cell paper.

UCSF Genentech Fellowship and the American Heart Association Predoctoral Fellowship for funding my thesis work. The National Institutes of Health for funding the Mullins lab.

My dear friends, especially Megan Bergkessel, for teaching me everything I know about mountaineering and including me in countless adventures. May your paths be crooked and interesting, and your summits plentiful.

My brother, Andrew Zuchero, who would have dragged my body down from Doi Chang Dao for a proper burial had I expired in the night, and who has dragged me to far better places. The sun from underwater. The Milky Way above Tulum.

Dyche Mullins, my thesis advisor, and favorite squash opponent to best. He is one of the most brilliant scientists I have met, and I am incredibly grateful for all he has given me. He has crafted a unique lab culture that prizes meticulous and exciting science, independence, community—family, really—and wide-ranging interests. He has given me incredible opportunities to grow as a person and a scientist, not the least of which has been the ability to wallow in biology at Woods Hole. It has been a wild ride to be a part of the blossoming of the Mullins lab, and I would not have done it any other way.

Joy Yu, for your love, friendship, and companionship. Thank you for everything: too numerous to list and too boundless for words.

My parents, John and Sandra Zuchero, for showing me the world beyond the backwoods of Pennsylvania; for believing that sending me to a diverse, small, liberal, liberal arts college would be a useful investment in my future; for making that investment; for supporting and encouraging me to follow my dreams and my gut; for being two of the absolute greatest human beings on the planet; and for always having something interesting and delicious on the table.

Acknowledgements (Published Materials)

Part of this thesis was previously published in the journal *Nature Cell Biology* 11 (2009) and are reproduced from Nature Press, copyright 2009. Additional authors listed on this manuscript include: (1) Margot E. Quinlan, who conceived the N-WASp + MBL gain of function experiment for Spire, and generously contributed these data to the paper. (2-3) Amanda S. Coutts and Nicholas La Thangue, who contributed images of GFP-JMY expressed in U2OS cells, the RNAi scratch wounding motility experiments, and helped conceive the experiments and write the paper. (4) R. Dyrche Mullins directed and supervised the project and lab, and contributed ideas and his writing expertise.

**Regulation of Actin Polymerization by JMY:
Nucleation of Filaments
and Activation of the Arp2/3 Complex
to Control Cell Motility**

J. Bradley Zuchero

Abstract

Polymerization of actin into filaments powers diverse cellular functions, and a key way that cells build distinct types of actin networks is by using different actin nucleation factors. We identified a new vertebrate actin nucleation factor, junction-mediating and regulatory protein (JMY). JMY combines *de novo* nucleation by a Spire-like mechanism with activation of the Arp2/3 complex to rapidly generate branched actin networks. JMY localizes to the leading edge of motile cells, and contributes to cell motility. Since the Arp2/3 complex requires pre-existing filaments for its branching nucleation activity, we hypothesize that JMY contributes to cell motility by nucleating filaments, which then serve as substrates for JMY-activated Arp2/3 nucleation.

Table of Contents

Preface	Title Page	i
	Acknowledgements	iii
	Published Material.....	vii
	Abstract.....	viii
	Table of Contents.....	ix
	List of Figures.....	x
Chapter 1	Introduction	1
Chapter 2	p53-Cofactor JMY is a Multifunctional Actin	6
	Nucleation Factor	
	UCSF Library Release Form	54

List of Figures

Chapter 2	Figure 1	43
	Figure 2	44
	Figure 3	45
	Figure 4	46
	Figure 5	47
	Supplementary Figure 1	48
	Supplementary Figure 2	49
	Supplementary Figure 3	50
	Supplementary Figure 4	51
	Supplementary Figure 5	52
	Supplementary Figure 6	53

Chapter 1

Introduction

The actin cytoskeleton is essential to all eukaryotic cells. In addition to playing important structural roles, assembly of actin into filaments powers diverse cellular processes, including cell motility and endocytosis. Actin polymerization is tightly regulated by various cofactors, which control the spatial and temporal assembly of actin as well as the physical properties of these filaments

Over the past few decades dozens of actin binding proteins have been discovered, and there is a rapidly growing body of work focused on dissecting how each of these proteins regulates the kinetics and morphology of actin structures (1). Actin dynamics can be divided into three steps, each of which is specifically regulated. Polymerization is a nucleation-condensation reaction (2), which means that the first step (nucleation) is slow, and the second step (elongation) proceeds quickly once a stable nucleus is formed (3). Nucleation refers to the assembly of actin monomers into a stable trimer, which is usually an extremely unfavorable reaction. As the filament elongates, incorporated actin monomers hydrolyze their ATP to ADP, making filaments more susceptible to depolymerization, the third step in the cycle. All steps of this cycle are regulated by actin binding proteins (1). The rate of nucleation is controlled by three distinct classes of actin nucleators: the Arp2/3 complex (4), formins and spire/WH2 nucleation factors (5, 6). This final class is rapidly expanding, and includes putative nucleation factors like Cordon Bleu (7), leiomodin (8), and several bacterial and viral actin nucleators (9). Although the mechanism of nucleation might be different for each of these proteins, the common thread is the use of a tandem array of actin monomer-binding WASp Homology 2 (WH2) domains,

usually three or four in short succession. Each WH2 domain is thought to bind to an actin monomer, stitching together a filament nucleus that can then rapidly elongate (6, 7).

We identified a novel, vertebrate-specific actin nucleation factor called JMY, with homology to both Spire as well as Arp2/3 activators like N-WASp and Scar. Chapter 2 details our initial biochemical and cell biological characterization of JMY. We find that JMY nucleates actin by a Spire-like mechanism, and also activates the Arp2/3 complex by a N-WASp-like mechanism. Endogenous JMY is nuclear in most cells, but shifts to a cytoplasmic, leading edge-enriched localization in highly motile cells. Consistent with this motility-dependent change in localization, JMY is important for cell migration. We propose that JMY builds actin networks required for cell motility by “jump-starting” Arp2/3-dependent filament branching: first by nucleating mother filaments, and then by activating Arp2/3 to branch off of these.

JMY was originally identified as a coactivator of p53, and is known to accumulate in the nucleus following DNA damage. Does JMY promote actin polymerization in the nucleus as part of its role in regulating transcription? Experiments to test the role of actin nucleation by JMY in the nucleus are confounded by the fact that actin binding regulates subcellular localization of JMY (Zuchero and Mullins, unpublished observations). To overcome this technical hurdle, I have engineered mutant constructs of JMY with a triplicate repeat of exogenous SV-40 nuclear localization signals. It would be interesting to test whether, when coexpressed with p53, these versions of JMY unable to bind

actin or the Arp2/3 complex are able to stimulate p53-dependent transcription and apoptosis to the same degree as wild-type JMY. I leave these experiments to the next generation.

References

1. Pollard, T.D. and Borisy, G.G. (2003) Cellular motility driven by assembly and disassembly of actin filaments. *Cell* **112**, 453--465.
2. Oosawa, F. and Kasai, M. (1962) A theory of linear and helical aggregations of macromolecules. *J Mol Biol.* **4**, 10--21.
3. Frieden C. (1983) Polymerization of actin: mechanism of the Mg²⁺-induced process at pH 8 and 20 degrees C. *Proc Natl Acad Sci U S A.* **80**, 6513--6517.
4. Welch, M.D. and Mullins, R.D. (2002) Cellular control of actin nucleation. *Annu Rev Cell Dev Biol.* **18**, 247--288.
5. Baum, B. and Kunda, P. (2005) Actin nucleation: spire - actin nucleator in a class of its own. *Curr Biol.* **15**, R305--R308.
6. Quinlan, M.E., Heuser, J.E., Kerkhoff, E. and Mullins, R.D. (2005) Drosophila Spire is an actin nucleation factor. *Nature* **433**, 382--388.
7. Ahuja, R., Pinyol, R., Reichenbach, N., Custer, L., Klingensmith, J., Kessels, M.M. and Qualmann, B. (2007) Cordon-bleu is an actin nucleation factor and controls neuronal morphology. *Cell.* **131**, 337-50.
8. Chereau, D., Boczkowska, M., Skwarek-Maruszewska, A., Fujiwara, I., Hayes, D.B., Rebowski, G., Lappalainen, P., Pollard, T.D. and Dominguez, R. (2008) Leiomodin is an actin filament nucleator in muscle cells. *Science* **320**, 239-43.
9. Qualmann, B. and Kessels, M.M. (2009) New players in actin polymerization--WH2-domain-containing actin nucleators. *Trends Cell Biol.* **19**, 276-85.

Chapter 2

p53-cofactor JMY is a Multifunctional Actin Nucleation Factor

Abstract

Many cellular structures are assembled from networks of actin filaments and the architecture of these networks depends on the mechanism by which the filaments are formed. Several classes of proteins are known to assemble new filaments, including the Arp2/3 complex, which creates branched filament networks, and Spire, which creates unbranched filaments^{1,2}. We find that JMY, a vertebrate protein first identified as a transcriptional co-activator of p53, combines these two nucleating activities by both activating Arp2/3 and assembling filaments directly using a Spire-like mechanism. Increased levels of JMY expression enhance motility while loss of JMY slows cell migration. When slowly migrating HL-60 cells are differentiated into highly motile neutrophil-like cells, JMY moves from the nucleus to the cytoplasm, and is concentrated at the leading edge. Thus, JMY represents a new class of multifunctional actin assembly factor whose activity is regulated, at least in part, by sequestration in the nucleus.

Results

By searching genome databases for sequences related to the WASp Homology 2 (WH2) domain we discovered a potential Arp2/3-activating sequence, WWWCA, in the vertebrate protein JMY (Fig. 1a). This sequence is composed of three tandem repeats of the actin monomer-binding WH2 domain (WWW); an actin- and Arp2/3-binding central domain (C); and an Arp2/3-binding acidic domain (A). These sequence elements, first identified in WASp-family

proteins^{1, 3}, collaborate in activating Arp2/3. The identification of these elements in JMY was surprising, since JMY localizes primarily to the nucleus and was originally discovered as a binding partner of p300, a coactivator for many transcription factors, including the tumour-suppressor p53⁴. In fibroblasts JMY accumulates in the nucleus in response to DNA damage, where it enhances p53-dependent transcription of pro-apoptotic genes^{4, 5}.

JMY nucleates actin filaments and activates the Arp2/3 complex

To determine whether JMY also plays a role in assembly of the actin cytoskeleton we tested the effect of JMY expression on actin organization *in vivo*. Overexpression of JMY in human U2OS cells induces formation of elongated actin filament structures that colocalize with JMY (Fig. 1b), similar to overexpression of WASp-family proteins and the actin nucleation factor Spire^{2, 6}. Truncation mutants demonstrate that the WH2 cluster is required for this effect but, curiously, the Arp2/3-binding CA domain is not (Supplementary Fig. S1). Expression of the C-terminal region of JMY fused to GFP (GFP-PWWWCA) produces a linear, dose-dependent increase in the cellular concentration of filamentous actin (Fig. 1c) as judged by correlating Alexa-568 phalloidin staining with GFP fluorescence (n=457; Fig. 1d). In contrast, expressing GFP alone has no significant effect on cellular levels of filamentous actin (n=458; Fig. 1d, Supplementary Fig. S1).

To study how JMY affects actin assembly *in vitro*, we first verified that all three putative WH2 domains (W_a, W_b, and W_c, from N- to C-terminal) bind monomeric actin (Supplementary Fig. S2). JMY activates Arp2/3 *in vitro*, as

determined by pyrene-actin polymerization assays using a C-terminal fragment of JMY (WWWCA) (Fig. 1e; $t_{1/2}$ (JMY + actin + Arp2/3) = 42.2 ± 2.3 s; versus $t_{1/2}$ (actin + Arp2/3) = 1193 ± 28 s). JMY WWWCA also induces rapid actin polymerization in the absence of Arp2/3 (Fig. 1e; $t_{1/2}$ = 188.5 ± 4.4 s). The JMY-dependent increase in polymerization rate is dose-dependent, both with and without Arp2/3 (Fig. 1f). This result is quite surprising and distinguishes JMY from all other proteins known to activate Arp2/3. N-WASp WWCA, for example, activates Arp2/3 to a similar extent as JMY, but does not accelerate polymerization in the absence of Arp2/3 (Fig. 1e).

By itself JMY could accelerate actin assembly by: (1) nucleating new filaments, (2) increasing the rate of filament elongation, or (3) severing existing filaments to create new barbed ends^{2, 7}. JMY does not affect elongation of preformed filaments, arguing that it neither accelerates elongation nor severs, but rather nucleates new filaments (Supplementary Fig. S3a-c). Indeed, we observe greater than 12-fold more filaments in the presence of JMY WWWCA compared to actin alone (Fig. 2a-b). In the presence of Arp2/3, JMY WWWCA produces branched filaments, consistent with nucleation by Arp2/3 (Fig. 2c, left panel), while, by itself, JMY nucleates unbranched filaments (Fig. 2a). In assembly reactions filament length is inversely proportional to the rate of nucleation, and filaments made in the presence of JMY are shorter than those made with actin alone. Arp2/3-nucleated filaments are even shorter (Fig. 2d). JMY produces twice as many branches per micron as Scar1/WAVE1 (Fig. 2e), consistent with JMY inducing a faster rate of Arp2/3 activation than Scar.

Some proteins that cap barbed ends *in vivo* (e.g. capping protein) nucleate filaments that elongate from their pointed end *in vitro*⁸. To determine whether JMY caps barbed ends, we made filaments and depolymerized them in the presence of JMY WWCA. JMY does not inhibit disassembly, arguing that it does not cap barbed ends but promotes polymerization by nucleating new filaments that elongate from their barbed ends (Supplementary Fig. S3d, e). Direct nucleation appears to explain the unexpected ability of JMY to induce actin assembly *in vivo* in the absence of the Arp2/3-binding CA domain (Supplementary Fig. S1).

Dissecting nucleation and Arp2/3-activation domains

We hypothesized that, similar to Spire², JMY uses its tandem WH2 domains to nucleate new filaments. We tested the activity of constructs consisting of either all three WH2 domains (JMY WWW), or the two C-terminal WH2 domains (JMY W_bW_c). JMY WWW nucleates actin as well as WWWCA, indicating that the CA region plays no role in direct nucleation (Fig. 2f). Moreover, addition of Arp2/3 to JMY WWW does not further increase the rate of polymerization (Fig. 2f). As with Spire, the two C-terminal WH2 domains (JMY W_bW_c) are sufficient for nucleation, but all three JMY WH2 domains are required for maximal activity (Supplementary Fig. S3h, i).

In contrast, a fragment composed of a single WH2 domain (W_c) and the CA domains (JMY WCA) activates Arp2/3, but does not nucleate filaments on its own (Fig. 2g). JMY contains a conserved tryptophan residue known to be important for Arp2/3 binding in all WASp family proteins¹⁰. Replacing this

tryptophan with an alanine in JMY decreases activation of Arp2/3 without affecting intrinsic nucleation activity (Supplementary Fig. S3j). These results argue that nucleation and Arp2/3 activation are separable activities, and that JMY activates Arp2/3 by the same mechanism as WASp-family proteins.

Nucleation by a Spire-like mechanism

Similarities in the sequences and activities of JMY and Spire suggested that the two proteins nucleate filaments by a common mechanism. We compared the kinetics of nucleation by JMY and Spire over a range of actin concentrations. At all concentrations of actin tested, JMY and Spire display nearly identical kinetics (Supplementary Fig. S3k-l). Also, similar to Spire, high concentrations of JMY sequester actin monomers (Supplementary Fig. S3m-n). Unlike Spire, however, JMY WWCA does not prevent dissociation of monomers from the pointed end of filaments (Supplementary Fig. S3f-g). It is possible that the full-length JMY interacts with filament ends, but this is not required for nucleation.

Spire nucleates actin by stitching monomers together using tandem WH2 domains and a novel actin binding motif (previously called “Linker 3”²) that we designate the Monomer Binding Linker, or MBL. Spire-MBL, a short (~15 AA) sequence connecting the third and fourth WH2 domains, is sufficient to promote weak nucleation². We compared the sequences of Spire-MBL with the region between the two C-terminal WH2 domains of JMY (W_b and W_c) and N-WASp. Most residues conserved between Spire homologs are also conserved in JMY, but not in N-WASp (Fig. 3a). Another WH2-containing nucleation factor, Cordon Bleu (Cobl), is thought to operate by a different mechanism¹¹ and, consistent with

this, we see no conservation between the linker regions of Cobl and Spire (Fig. 3a).

Do JMY and Spire nucleate actin by the same mechanism? We replaced the JMY linker with a set of glycine-serine repeats (JMY $W_bW_c(\text{gs}5)$), and compared it to a similar Spire mutant (Spire CD($\text{gs}5$)). JMY $W_bW_c(\text{gs}5)$ has a modest defect in nucleation, while replacing the linker in Spire has a more pronounced effect (Fig. 3b, d; Supplementary Fig. S3o). Interestingly, inserting either the JMY- or Spire-MBL between the N-WASp WH2 domains (NW WJW or WSW) converts N-WASp into a nucleator (Fig. 3c,d, Supplementary Fig. S3p), while inserting a flexible linker (NW WW($\text{gs}5$)) does not (Fig. 3b,d). NW WJW and WSW do not nucleate as well as JMY or Spire. Thus, nucleation by JMY and Spire requires unique properties of both the linker (MBL) and the WH2 domains (Fig. 3e).

From the nucleus to the leading edge

To investigate its role in actin assembly *in vivo*, we determined the localization of JMY in multiple cell types. JMY is primarily nuclear in mouse embryonic fibroblasts, B16-F10 mouse melanoma cells, NIH 3T3 cells, and primary rat neurons (Supplementary Fig. S4 and data not shown). In ruffling B16-F10 cells, we observe a small fraction of JMY colocalized with actin filaments at the leading edge (Supplementary Fig. S4b). Interestingly, in highly motile, primary human neutrophils, JMY is almost entirely excluded from the nucleus, and colocalizes with filaments at the leading edge (Fig. 4d). JMY does not bind

actin filaments *in vitro*, so this localization does not simply reflect direct interaction of JMY with filaments (Supplementary Fig. S4d).

Our localization studies suggest that JMY's presence at the leading edge correlates with motility. To further test this we investigated JMY expression and localization in HL-60 cells, which can exist as non-motile, relatively undifferentiated cells or be induced to differentiate into highly motile cells¹². In undifferentiated HL-60 cells, JMY is primarily nuclear, and does not colocalize with filaments (primarily nuclear in 91% of cells, n=246; Fig. 4a, Supplementary Fig. 5). Addition of 1.3% DMSO to the culture medium induces differentiation into highly motile cells that polarize and undergo chemotaxis. During differentiation JMY localization shifts dramatically, becoming almost entirely cytoplasmic. This shift occurs approximately 2 days before cells are competent to polarize in response to chemoattractant (fMLP; Supplementary Fig. S5c). In differentiated cells JMY colocalizes with filamentous actin in the cell cortex (cytoplasmic in 94%, nuclear in 6%, n=212; Fig. 4b), and upon addition of fMLP, JMY localizes strongly to the leading edge where it overlaps with filamentous actin (88% of polarized cells, n=311; Fig. 4c, Supplementary Fig. S5d). Comparing JMY staining to soluble GFP in polarized cells shows that enrichment of JMY at the leading edge is not a volume artefact (Supplementary Fig. S5e-g). These data suggest that translocation of JMY to the cytosol plays a role in building the leading edge. Interestingly, expression of JMY's nuclear binding partner p300 disappears when HL-60 cells are differentiated, suggesting that the nuclear

(p300/p53-dependent transcription) and cytoplasmic (actin nucleation) roles of JMY are regulated by separate pathways (Fig. 4e).

JMY contributes to cell motility

To test JMY's role in cell motility, we stably expressed GFP-JMY and GFP-JMY Δ CA in U2OS cells, grew monolayers, scratched them, and monitored wound healing over time¹³. Cells expressing GFP-JMY migrate 17% faster than wild-type cells (n=3; p<0.003; Fig. 5a-b, Supplementary Fig. S6). In contrast, cells expressing GFP-JMY Δ CA migrate at the same rate as wild-type cells (GFP-JMY, 43.8 \pm 1.6 μ m/hr; GFP-JMY Δ CA, 38.5 \pm 1.7 μ m/hr; wild-type, 37.5 \pm 1.0 μ m/hr), suggesting that JMY requires its Arp2/3-activating activity to enhance motility.

We next knocked-down JMY expression in cultured U2OS and HEK 293 cells by RNAi. Western blotting shows that RNAi was efficient (Fig. 5e, Supplementary Fig. S6). In both cell lines knock-down of JMY expression significantly slows the rate of wound healing (Fig. 5c-d, Supplementary Fig. S6). In the first 6 hours, cells treated with JMY siRNA move 38.0% slower than control U2OS cells (n=4; p<0.05). By 24 hours, control cells fully migrate into the wound, whereas cells treated with JMY siRNA migrate only 86 percent of the distance (Fig. 5a-b; n=4). Control HEK 293 cells migrate 92 percent of the distance by 24 hours, whereas cells treated with JMY siRNA migrate 60 percent (Supplementary Fig. S6; n=7).

Defects in wound healing could be caused by: (1) reduced actin assembly, (2) altered transcription, (3) reduced cell division or increased apoptosis, or (4)

off-target effects of the siRNA. Consistent with (1), we find that JMY-knockdown cells contain $11.4 \pm 0.4\%$ ($n=396$, $p<0.03$) less filamentous actin than wild-type cells (Fig. 5f). Loss of either p53 or p300, which are required for all JMY's known transcriptional effects, leads to increased cell migration¹⁴⁻¹⁶, inconsistent with transcriptional effects on motility. In addition, less than 5% of cells close to the wound divide in the first 6 hours of the assay, making it unlikely that cell division contributes to the observed defect. Knockdown of JMY was shown to decrease apoptosis⁵, ruling out explanation (3). To address possible off-target effects, we used three different siRNAs, from different regions of the human JMY gene, to knock down expression in HEK 293 cells. All three caused migration defects (Supplementary Fig. S6g), while a control siRNA had no effect.

We next tested whether JMY localizes to the leading edge of U2OS cells during migration in response to a wound, as seen in highly motile HL-60 cells. We fixed and stained U2OS cells 15 minutes after wounding, as well as cells in a sub-confluent and non-wounded cultures. Although the majority of JMY is nuclear in these cells, we also observe both endogenous JMY and GFP-JMY colocalized with filamentous actin at the leading edge, (Fig. 5g, Supplementary Fig. S4c), both in cells adjacent to a wound and in ruffling edges of sub-confluent cells (data not shown). Thus, even in cells where JMY is predominantly nuclear, a fraction of the protein can influence actin assembly at the leading edge and promote migration.

Role of JMY-dependent actin polymerization

JMY combines an unusual set of activities. The combination of transcriptional coactivation and actin nucleation activities suggests that JMY might mediate cellular decisions involving apoptosis and migration. Alternatively, JMY might be a chimera whose transcriptional and cytoskeletal functions are more or less independent. More intriguing is JMY's combination of Arp2/3-dependent and independent nucleation activities. A cell switching from a resting to a motile state must extensively remodel its cytoskeleton¹⁷. The leading edge of most migrating cells is characterized by a highly-branched dendritic arbour of actin filaments nucleated by Arp2/3, and one requirement for generating such a network is the pre-existence of "mother" filaments for Arp2/3 to bind and branch from^{18,19}. Although resting cells contain some actin filaments (cortical actin, stress fibres, etc.) recent work suggests that not all filaments can serve as efficient substrates for Arp2/3-dependent nucleation^{20, 21}. We hypothesize that JMY contributes to cell motility by nucleating filaments to jump-start Arp2/3-dependent nucleation and branching. By first nucleating new mother filaments and then activating Arp2/3 to branch off of these filaments, JMY could promote the rapid formation of a branched actin network. It is also possible that JMY has evolved to promote actin polymerization in different cellular contexts: (1) in the cytoplasm in the presence of Arp2/3, or (2) in the nucleus in the absence of Arp2/3 (see model in Fig. 5h). For example, it would be interesting to test whether inactivation of JMY's function in actin dynamics affects its role as a p300-dependent transcriptional coactivator for p53. Future work is aimed at testing these models.

Acknowledgements

This work was supported by grants from the NIH, the American Heart Association Predoctoral Fellowship (JBZ), MRC-Funding (ASC), and the Burroughs-Wellcome Fund Career Award in the Biomedical Sciences Fellowship (MEQ). We thank A. Kelly and R. Manlove for sequence analysis; O. Akin for help with Matlab scripts and advice; C. Campbell and H. Bourne for critical reading of the manuscript; O. Weiner, S. Wilson, P. Temkin, E. Oh, C. Vizcarra, S. Cai, M. D'Ambrosio, K. Campellone, and members of the Mullins lab for reagents and helpful discussions.

References

1. Welch, M. & Mullins, R. Cellular control of actin nucleation. *Annu Rev Cell Dev Biol* **18**, 247-88 (2002).
2. Quinlan, M. E., Heuser, J. E., Kerkhoff, E. & Mullins, R. D. Drosophila Spire is an actin nucleation factor. *Nature* **433**, 382-8 (2005).
3. Marchand, J. B., Kaiser, D. A., Pollard, T. D. & Higgs, H. N. Interaction of WASP/Scar proteins with actin and vertebrate Arp2/3 complex. *Nat Cell Biol* **3**, 76-82 (2001).
4. Shikama, N. et al. A novel cofactor for p300 that regulates the p53 response. *Mol Cell* **4**, 365-76 (1999).
5. Coutts, A., Boulahbel, H., Graham, A. & La Thangue, N. Mdm2 targets the p53 transcription cofactor JMY for degradation. *EMBO Rep.* **8**, 84-90 (2006).
6. Symons, M. et al. Wiskott-Aldrich syndrome protein, a novel effector for the GTPase CDC42Hs, is implicated in actin polymerization. *Cell* **84**, 723-34 (1996).
7. Pollard, T. & Borisy, G. Cellular motility driven by assembly and disassembly of actin filaments. *Cell* **112**, 453-65 (2003).
8. Cooper, J. & Pollard, T. Effect of capping protein on the kinetics of actin polymerization. *Biochemistry* **24**, 793-9 (1985).
9. Pollard, T. D. & Cooper, J. A. Quantitative analysis of the effect of Acanthamoeba profilin on actin filament nucleation and elongation. *Biochemistry* **23**, 6631-41 (1984).

10. Pan, F., Egile, C., Lipkin, T. & Li, R. ARPC1/Arc40 mediates the interaction of the actin-related protein 2 and 3 complex with Wiskott-Aldrich syndrome protein family activators. *J Biol Chem* **279**, 54629-54636 (2004).
11. Ahuja, R. et al. Cordon-Bleu Is an Actin Nucleation Factor and Controls Neuronal Morphology. *Cell* **131**, 337-350 (2007).
12. Collins, S., Ruscetti, F., Gallagher, R. & Gallo, R. Normal functional characteristics of cultured human promyelocytic leukemia cells (HL-60) after induction of differentiation by dimethylsulfoxide. *J Exp Med* **149**, 969-74 (1979).
13. Kowalski, J. R. et al. Cortactin regulates cell migration through activation of N-WASP. *J Cell Sci* **118**, 79-87 (2005).
14. Sablina, A., Chumakov, P. & Kopnin, B. Tumor suppressor p53 and its homologue p73alpha affect cell migration. *J Biol Chem* **278**, 27362-71 (2003).
15. Gadea, G., de Toledo, M., Anguille, C. & Roux, P. Loss of p53 promotes RhoA-ROCK-dependent cell migration and invasion in 3D matrices. *J Cell Biol* **178**, 23-30 (2007).
16. Krubasik, D. et al. Absence of p300 induces cellular phenotypic changes characteristic of epithelial to mesenchyme transition. *Br J Cancer* **94**, 1326-32 (2006).
17. Southwick, F. S., Dabiri, G. A., Paschetto, M. & Zigmond, S. H. Polymorphonuclear leukocyte adherence induces actin polymerization by a transduction pathway which differs from that used by chemoattractants. *J Cell Biol* **109**, 1561-9 (1989).

18. Mullins, R., Heuser, J. & Pollard, T. The interaction of Arp2/3 complex with actin: nucleation, high affinity pointed end capping, and formation of branching networks of filaments. *Proc Natl Acad Sci U.S.A.* **95**, 6181-6 (1998).
19. Blanchoin, L. et al. Direct observation of dendritic actin filament networks nucleated by Arp2/3 complex and WASP/Scar proteins. *Nature* **404**, 1007-11 (2000).
20. Blanchoin, L., Pollard, T. D. & Hitchcock-DeGregori, S. E. Inhibition of the Arp2/3 complex-nucleated actin polymerization and branch formation by tropomyosin. *Curr Biol* **11**, 1300-4 (2001).
21. Shao, D., Forge, A., Munro, P. & Bailly, M. Arp2/3 complex-mediated actin polymerisation occurs on specific pre-existing networks in cells and requires spatial restriction to sustain functional lamellipod extension. *Cell Motil Cytoskeleton* **63**, 395-414 (2006).
22. Quinlan, M., Hilgert, S., Bedrossian, A., Mullins, R. & Kerkhoff, E. Regulatory interactions between two actin nucleators, Spire and Cappuccino. *J Cell Biol* **179**, 117-28 (2007).
23. Gordon, D. J., Eisenberg, E. & Korn, E. D. Characterization of cytoplasmic actin isolated from *Acanthamoeba castellanii* by a new method. *J Biol Chem* **251**, 4778-86 (1976).
24. Cooper, J. A., Walker, S. B. & Pollard, T. D. Pyrene actin: documentation of the validity of a sensitive assay for actin polymerization. *J Muscle Res Cell Motil* **4**, 253-62 (1983).

25. Dayel, M. J., Holleran, E. A. & Mullins, R. D. Arp2/3 complex requires hydrolyzable ATP for nucleation of new actin filaments. *Proc Natl Acad Sci U S A* **98**, 14871-6 (2001).
26. Pollard, T. D. Rate constants for the reactions of ATP- and ADP-actin with the ends of actin filaments. *J Cell Biol* **103**, 2747-54 (1986).
27. Akin, O. & Mullins, R. D. Capping protein increases the rate of actin-based motility by promoting filament nucleation by the Arp2/3 complex. *Cell* **133**, 841-51 (2008).
28. Weiner, O. et al. Hem-1 complexes are essential for Rac activation, actin polymerization, and myosin regulation during neutrophil chemotaxis. *PLoS Biol* **4**, e38 (2006).
29. Cassimeris, L., McNeill, H. & Zigmond, S. Chemoattractant-stimulated polymorphonuclear leukocytes contain two populations of actin filaments that differ in their spatial distributions and relative stabilities. *J Cell Biol* **110**, 1067-75 (1990).
30. Stuurman, N., Amodaj N., Vale, R.D. Micro-Manager: Open Source software for light microscope imaging. *Microscopy Today* **15**, 42-43 (2007).
31. Petrella, E., Machesky, L., Kaiser, D. & Pollard, T. Structural requirements and thermodynamics of the interaction of proline peptides with profilin. *Biochemistry* **35**, 16535-43 (1996).
32. Kelly, A., Kranitz, H., Dötsch, V. & Mullins, R. Actin binding to the central domain of WASP/Scar proteins plays a critical role in the activation of the Arp2/3 complex. *J Biol Chem* **281**, 10589-97 (2006).

33. Kreishman-Deitrick, M. et al. NMR analyses of the activation of the Arp2/3 complex by neuronal Wiskott-Aldrich syndrome protein. *Biochemistry* **44**, 15247-56 (2005).
34. Campellone, K. G., Webb, N. J., Znameroski, E. A. & Welch, M. D. WHAMM is an Arp2/3 complex activator that binds microtubules and functions in ER to Golgi transport. *Cell* **134**, 148-61 (2008).

Experimental Procedures

Molecular Biology and Biochemistry. Constructs were cloned from full length mouse JMY⁴, fly Spire², and rat N-WASp using standard techniques. Primer sequences are available upon request. All constructs were sequenced to ensure no mutations were introduced during cloning. JMY fragments were expressed as GST-fusions in *E. coli* and purified using a combination of glutathione and cation chromatography. Except for individual WH2 domains, the GST was removed to prevent dimerization of the recombinant protein, which results in a marked increase in the rate of both intrinsic nucleation and activation of Arp2/3 (data not shown). To improve reproducibility of fluorimetry reactions, we mutated the non-conserved cysteine C978 to serine. This mutation does not change the kinetics of activation of Arp2/3 (Supplementary Fig. S6h, i), but is more stable than wild-type peptide. JMY concentrations were calculated using predicted molar extinction coefficients for JMY peptides that contained tryptophan residues (ProtParam), or by quantitative SDS-PAGE with Sypro-Red staining (Invitrogen). Amino acid numbers (mouse JMY, fly Spire, rat N-WASp) of constructs are: W_a, 853-876; W_b, 883-907; W_c, 913-938; WWWCA, 853-983; WWCA, 883-983; WCA, 906-983; W_bW_c, 883-938; W_aW_bW_c, 819-938; Spire CD, 428-482; N-WASp WWCA, 400-501; N-WASp WW, 400-450; GFP- and HA-JMY, 1-983; GFP-JMY Δ CA, 1-938; GFP-JMY Δ WWWCA, 1-852 (Supplementary Fig. S7).

Actin biochemistry assays. Actin was purified from *Acanthamoeba castellanii* as described²³, labelled with pyrene iodoacetamide as described²⁴, and stored on ice. Arp2/3 was purified from *Acanthamoeba* as described²⁵ and flash frozen with

10% glycerol. For all assays, Arp2/3 was thawed daily and diluted with 1 mg/mL BSA in Buffer A (0.2 mM ATP, 0.5 mM TCEP, 0.1 mM CaCl₂, 0.02% w/v sodium azide, 2 mM Tris, pH 8.0 at 4°C). Actin polymerization assays were performed in 1x KMEI (50 mM KCl, 1 mM MgCl₂, 1 mM EGTA, 10 mM imidazole, pH 7.0). Ca²⁺-actin was converted into Mg²⁺-actin by incubation of actin in ME (50 mM MgCl₂, 0.2mM EGTA) for two minutes prior to adding 10x KMEI and test components. Pyrene fluorescence was measured with an ISS PCI/K2 fluorimeter. Unless otherwise noted, polymerization reactions contained 2 μM actin (5% pyrene labelled), 2.5 nM Arp2/3 and 167 nM JMY or N-WASp. JMY proteins were diluted with 10 mg/mL BSA in Buffer A to prevent loss of activity. To normalize fluorimetry data, we subtracted the offset from zero then divided by the plateau value of actin alone, so as to not mask the effects of sequestration by JMY. For half-time calculations, reactions were normalized by dividing by their own plateau and solving for time at half-maximal fluorescence (0.5 a.u.).

To visualize actin filaments we polymerized 2 μM actin under the same conditions used for fluorimetry, then arrested reactions at the time indicated with Alexa Fluor 488 phalloidin and Latrunculin B. This technique preserves the ratio of monomeric to filamentous actin at the moment of quenching²⁷. To keep the concentration of F-actin constant we arrested reactions at their individual t^{9/10}s: 1 m 40 s for JMY+Arp2/3; 6 m 20 s for Scar+Arp2/3; 37 m 0 s for actin alone. Filaments were diluted to low nanomolar concentrations and spotted on poly-L-lysine (Sigma) coverslips, using wide-bore pipette tips to minimize shearing.

For actin filament cosedimentation assays, we expressed His-tagged full length JMY in *E. coli*, purified it by affinity chromatography, and performed actin filament cosedimentation assays as described in Quinlan et al. (2007)²² with minor modifications. Briefly, 4 μ M actin was polymerized in 1x KMEI, 20 μ g/mL BSA (loading control), and 1 mM DTT for one hour. An equal volume of serial dilutions of full length JMY was added to the actin. JMY was pre-cleared by centrifugation at 100,000 g for 20 min at 4° C before each assay. Samples were mixed, held on ice for 10 min, and pelleted at 100,000 g for 30 min at 4° C. Supernatants were removed, pellets were washed before resuspending, and each was analyzed by SDS-PAGE. We used SyproRed staining (Invitrogen) and quantified gels using a multiformat imager (Typhoon 9400, GE Healthcare) and ImageQuant software (GE Healthcare).

Depolymerization and critical concentration assays were performed as described.² Briefly, for barbed end depolymerization, we polymerized 5 μ M actin (40% pyrene labelled) for at least one hour. To stimulate depolymerization, we diluted these filaments tenfold (to 500 nM) in 1x KMEI containing the proteins to be tested. Depolymerization is due to filaments disassembling until they reach a new steady state. Under these conditions depolymerization proceeds both from the barbed and pointed ends but dissociation of monomers from the barbed end is roughly 25 times faster than from the pointed end (ADP actin). The depolymerization rate we measure is, therefore, mostly dependent on the kinetics of the barbed end.

For pointed-end depolymerization experiments we made gelsolin-actin seeds by mixing 24 μM actin, 12 μM gelsolin, and 10 mM CaCl_2 in Buffer A and polymerizing for 4 hours at room temperature followed by incubation overnight at 4° C. The concentration of pointed ends was quantified by actin elongation experiments. We made labelled filaments with capped barbed ends by polymerizing 5 μM actin (40% pyrene labelled) in the presence of 30 nM gelsolin-actin seeds. To stimulate depolymerization, we diluted these capped filaments tenfold (to 500 nM) in 1x KMEI containing proteins to be tested. To ensure that filament barbed ends were capped, we measured depolymerization kinetics in the presence of 500 nM Arp2/3, which caps free pointed ends.

Elongation experiments were performed as described.² Briefly, seeds were prepared by polymerizing 4 μM unlabeled actin in 1x KMEI for 1 hour at 22°C. 4 μM actin (5% pyrene labelled) was then polymerized alone or in the presence of these actin filament seeds, with or without 500 nM JMY WWCA (as noted). Polymerization rates were calculated during the linear phase of the reactions, between 40 and 180 s.

Cell culture. U2OS (ATCC) and HEK 293 cells were cultured in Dulbecco's modified Eagle's medium supplemented with 10% FBS, 2 mM L-glutamine, non-essential amino acids, and penicillin-streptomycin (UCSF Cell Culture facility). For transfection, cells were seeded onto glass coverslips and transfected with HA-JMY⁴ using GeneJuice (Merck), or GFP-JMY and GFP-RNAi constructs using Lipofectamine LTX (Invitrogen), according to manufacturer's protocol. HL-60 cells were cultured as described²⁸, in RPMI-1640 with 25 mM HEPES, 2.0 g/L

NaHCO₃, 10% FBS, 1% antibiotic-antimycotic (Fisher), and were passaged every 3-4 days to a density of 0.2×10^6 cells/mL. Differentiation was in complete medium containing 1.3% DMSO (Hybrimax, Sigma). All cells were grown at 37° with 5% CO₂. Primary human neutrophils were obtained by finger pinprick as described²⁹.

Immunofluorescence of HL-60 cells was performed as described²⁸. Briefly, flamed coverslips were treated with 200 µg/mL bovine plasma fibronectin (Sigma) in PBS, washed with PBS, and blocked with 1.8% low endotoxin BSA (Sigma) in modified Hanks buffered saline solution (mHBSS: 150 mM NaCl, 4 mM KCl, 1 mM MgCl₂, 10 mM glucose, 20 mM HEPES, pH 7.4 at 22° C) for 5 minutes prior to adhering cells. Cells were pelleted and resuspended in BSA/mHBSS, and adhered to coverslips for 30-60 minutes at 37° C, then washed to remove unbound cells. Stimulation or mock stimulation was in BSA/mHBSS with 100 nM (HL-60s) or 20 nM (human neutrophils) fMLP, or DMSO (carrier), for 5 minutes at 22° C. Cells were fixed in 3.2% formaldehyde in cytoskeletal buffer (138 mM KCl, 3 mM MgCl₂, 2 mM EGTA, 320 mM sucrose, 10 mM HEPES, pH 7.2 at 22° C). For immunofluorescence of U2OS cells, cells were plated on flamed, fibronectin-coated coverslips, and fixed for 30 minutes in 3.2% formaldehyde in PBS. Cells were then permeabilized with 0.1% triton in PBS with 1.4 U/mL Alexa Fluor 568 phalloidin (Invitrogen) to stabilize and visualize filaments. For JMY immunolocalization, rabbit polyclonal JMY antibody 1289⁵ or Anti-HA antibody HA11 (Babco) was used at a 1:500 dilution. Alexa Fluor 488-labeled goat-anti-rabbit secondary (Invitrogen) was used at a 1:500

dilution. DAPI (Sigma) was used at 0.5 $\mu\text{g}/\text{mL}$. Samples were mounted with fluorescent mounting medium (DakoCytomation).

Epifluorescence and wide field images were acquired on a Nikon TE300 inverted microscope equipped with a Hamamatsu C4742-98 cooled CCD camera, with Simple PCI software (Compix), using 100x and 60x 1.4 NA Plan Apo objectives (Nikon), or with a 10x 0.6 NA Phase objective, using MicroManager software³⁰. For quantification of F-actin levels in cells expressing GFP-PWWWCA or GFP, micrographs were acquired with an IX Micro automated microscope, using identical illumination conditions. Cells were identified and outlined using ImageJ software, background was subtracted, and the average intensity in the red and green channels were measured. We used ImageJ (National Institutes of Health) and Adobe Photoshop (Adobe) for image analysis and contrast adjustment.

For wound healing experiments, cells were plated on marked coverslips at the same density, scratch wounded with a micropipette tip, washed to removed detached cells, and then given fresh medium and kept at 37°C during image acquisition. Stable lines of U2OS cells stably expressing GFP-JMY and variants were selected in 500 $\mu\text{g}/\text{mL}$ G418 for at least 3 weeks, then enriched by FACS (UCSF Flow Cytometry Core). siRNA was used at a final concentration of 25nM (hJMY siRNA from Santa Cruz and control non-targeting 2 from Dharmacon) and transfected into cells with oligofectamine or Dharmafect 1 (both according to manufacturer's protocols), and cells were grown for 72 hours prior to experiments. To discriminate between RNAi and non-RNAi cells, pL-UGIH plasmid (ATCC) was modified to contain a human JMY-specific hairpin based on

the sequence of JMY-specific siRNA-3 by the method of Weiner et al. (2006)²⁸. HEK 293 cells transiently transfected with this construct were grown for 7 days prior to fixation or immunoblotting.

Standard methods were used for Western blotting, using 1:500 1289 or 1:1000 L-16 (Santa Cruz Biotechnology) JMY primary antibodies and 1:5000 HRP-anti-rabbit secondary (Jackson ImmunoResearch). p300-CT primary antibody (Millipore) was used at 1:500, goat-anti human GAPDH (Santa Cruz) was used at 1:10,000, and mouse anti-human actin (Sigma) was used at 1:20,000. HRP secondaries (Dako) were used at 1:10,000, and ECL reagent (SuperSignal West Pico, Pierce) was used according to the manufacturer's instructions. All error values are standard error of the mean, s.e.m. We used two-tailed unpaired t-tests, assuming unequal variance, to calculate p-values (Microsoft Excel).

Figure Legends

Figure 1. JMY nucleates actin filaments and activates the Arp2/3 complex.

(a) Domain structure of JMY. The C-terminus of JMY is homologous to activators of Arp2/3. A poly-proline (P) domain³¹ is followed by three tandem actin monomer-binding WH2 domains (W_a through W_c), an actin and Arp2/3-binding central domain (C), and an Arp2/3-binding acidic domain (A). Alignment shows individual WH2 domains of JMY, and compares the sequences of the WCA regions of JMY, Scar, and N-WASp. JMY WCA is 28% identical to N-WASp WCA (ClustalW), and residues putatively involved in binding actin and Arp2/3^{32, 33} are 100% conserved between all available JMY sequences.

(b) Expression of HA-JMY (top panels; visualized by indirect immunofluorescence of HA, green) in U2OS cells induces the formation of filamentous actin structures (visualized with Alexa Fluor 568 phalloidin, red). These elongated actin structures colocalize with JMY and are not seen in untransfected cells (bottom panels). Nuclei were visualized with DAPI (blue). Scale bar, 10 μm .

(c) Expression of GFP-PWWWCA (green) in U2OS cells increases cellular F-actin (Alexa Fluor 568 phalloidin, red).

(d) Quantification of the increase in F-actin induced by GFP-PWWWCA expression. Phalloidin intensity was plotted as a function of GFP-PWWWCA intensity and shows a linear increase in F-actin content with increased expression of GFP-PWWWCA (n=457). In contrast, expressing GFP alone has

only a minor effect on the red intensity detected, likely due to a small amount of bleed-through (n=458).

(e) Pyrene-actin polymerization assays show that JMY WWWCA both activates Arp2/3 (R) and nucleates actin in the absence of Arp2/3 (red and blue traces). N-WASp (NW) WWCA activates Arp2/3 (green), but does not nucleate actin on its own (grey).

(f) Intrinsic nucleation and activation of Arp2/3 by WWWCA are dose-dependent. Pyrene-actin polymerization assays were conducted in the absence (blue) or presence (red) of Arp2/3, with increasing concentrations of JMY WWWCA. Time to half-maximal polymerization was plotted as a function of WWWCA concentration. Pyrene-actin polymerization assays were in 1x KMEI and contained 2 μ M actin, 167 nM JMY or N-WASp, and 2.5 nM Arp2/3, where noted.

Figure 2. Mechanistic dissection of JMY.

(a) JMY nucleates unbranched filaments, and increases the number of filaments over actin alone. Filaments made in the presence (left) or absence (right) of 167 nM JMY WWWCA were fixed with Alexa Fluor 488 phalloidin and Latrunculin B at 6 minutes ($t^{9/10}$ of JMY WWWCA reaction) prior to dilution and spotting on poly-L-lysine coverslips^{27,2}. Scale bars, 5 μ m.

(b) Quantification of filaments per field in images from **a** demonstrates that JMY nucleates new filaments (JMY, 42.7 ± 4.2 filaments per micron, n=35 fields; actin alone, 3.2 ± 0.5 filaments per micron, n=30 fields).

(c) Filaments prepared as in **a**, in the presence of JMY plus Arp2/3 (left), Scar plus Arp2/3 (centre), or actin alone (right). The concentration of filaments was kept constant by arresting reactions at their individual $t^{9/10}$ s (see Methods). Filaments nucleated in the presence of JMY and Arp2/3 are branched, consistent with JMY activating Arp2/3, as are filaments made in the presence of Scar and Arp2/3. The shorter, more abundant filaments seen here are due to Arp2/3 nucleating actin more rapidly than intrinsic nucleation by JMY.

(d) Quantification of filament length at $t^{9/10}$. The rate of nucleation is inversely proportional to the length of filament (rate: JMY+Arp2/3 > JMY > Scar+Arp2/3 >> actin alone).

(e) Quantification of filament branching in each condition. $n > 300$ filaments per condition.

(f) Tandem WH2 domains from JMY are sufficient for actin nucleation. Actin polymerization is as fast with WWW as it is with WWWCA. WWW lacks the Arp2/3 binding CA domain, so adding Arp2/3 to WWW does not accelerate polymerization over WWW alone. N-WASp WW does not nucleate actin.

(g) JMY WCA is sufficient to activate Arp2/3, but does not nucleate actin. The rate of actin polymerization in the presence of JMY WCA and Arp2/3 is similar to reactions containing Scar WCA and Arp2/3. In the absence of Arp2/3, JMY WCA has no effect on actin polymerization. Experimental conditions as in Fig. 1.

Figure 3. JMY nucleates actin by the same mechanism as Spire.

(a) The region between JMY W_b and W_c is homologous to the short actin nucleation motif from Spire (monomer-binding linker, MBL). The figure shows an alignment between Spire-MBL and the same region of JMY (mJMY AA 903-917) with homologous residues coloured grey. The MBL sequence is not homologous to the analogous position in N-WASp, WHAMM³⁴, or Cordon Bleu¹¹. The position of the glycine-serine repeats in **b** is underlined, and the sequences of N-WASp gain of function mutations (NW WJW and WSW) in **c** are shown.

(b) JMY-MBL is important for actin nucleation. Replacing the MBL in JMY W_bW_c and Spire CD (the two C-terminal WH2 domains in Spire) with a flexible linker of glycine-serine repeats (gs5) causes a nucleation defect in both JMY and Spire. The analogous N-WASp mutant does not promote nucleation, but inhibits spontaneous polymerization.

(c) Gain of function. Replacing the linker region between the WH2 domains of N-WASp WW with JMY- or Spire-MBL (NW WJW or WSW) converts N-WASp into a weak actin nucleator. This shows that JMY- and Spire-MBL are sufficient for nucleation. Mutated amino acids of WJW and WSW are shown in **a**. Reactions in **b** and **c** contained 4 μ M actin. Experimental conditions as in Fig. 1.

(d) $t/12s$ of reactions from b-c. Reactions were repeated > 3 times each. Error bars, s.e.m.

(e) Actin nucleation and activation of Arp2/3 are distinct activities of JMY that overlap spatially. Tandem JMY WH2 domains and the MBL (star in figure) nucleate actin, similar to Spire, and JMY WCA activates Arp2/3, similar to N-WASp and Scar.

Figure 4. JMY localizes to the leading edge of motile cells.

(a-c) Redistribution of JMY from the nucleus to the leading edge in HL-60 cells.

(a) JMY is primarily nuclear in undifferentiated HL-60 cells. (b) Following differentiation into motile cells by culturing in 1.3% DMSO for 5-7 days, JMY colocalizes with filamentous actin in the cytoplasm. (c) Differentiated HL-60 cells were polarized by exposure to 100 nM fMLP, a chemoattractant. JMY is distributed throughout the cytoplasm, where it colocalizes strongly with filamentous actin at the leading edge. Cells were fixed and stained with Alexa Fluor 568 phalloidin (red), anti-JMY (green), and DAPI (blue). Scale bars, 10 μ m.

(d) Human primary neutrophils were obtained by finger prick²⁹, stimulated with 20 nM fMLP, and fixed and stained as above. JMY (green) colocalizes with filamentous actin (red) at the leading edge. Scale bar, 5 μ m.

(e) Western blots of JMY and binding partner p300 in undifferentiated (U) and differentiated (D) HL-60 cells. p300 is expressed in undifferentiated, but not differentiated, HL-60 cells.

Figure 5. JMY contributes to cell motility.

(a-b) Expressing GFP-JMY in U2OS cells significantly increases their motility in wound healing assays. Stable lines of GFP-JMY and GFP-JMY Δ CA were wounded by scraping with micropipette tips. Images were acquired at 0, 2, 4, 6, and 12 hours after wounding. (b) Migration rate from 0-6 hours was averaged from a minimum of 4 replicates on each of 3 days. GFP-JMY expression induces

cells to migrate 16.6% faster than wild-type cells (n=3, p<0.003). Cells expressing a truncation of JMY lacking the Arp2/3-interacting CA domain migrate at the same rate as wild-type cells. Scale bars, 100 μ m.

(c-e) Wound healing assays in U2OS cells indicate that knocking-down JMY by RNAi impairs cell migration. Cells were transfected with JMY or control non-targeting 2 (Dharmacon) siRNA (C) and wounded (red dashed line) as in a. Images were taken at the same position 0, 3, 6, and 24 h after wounding. (d) Wound size at each time point for all conditions. (n=4). (e) Western blots show RNAi efficiency in U2OS cells.

(f) Knocking down JMY expression decreases cellular levels of F-actin. HEK 293 cells were transfected with a vector encoding both GFP and a JMY-specific shRNA²⁸ and fixed and stained with Alexa Fluor 568-phalloidin. Average phalloidin intensity in GFP-negative (non-RNAied) and GFP-positive (RNAied) cells is plotted (n=396, p<0.03, see Methods). Error bars, s.e.m.

(g) JMY localizes to the leading edge of U2OS cells. Cells were grown as above, and fixed and stained for JMY 15 minutes after wounding. JMY is primarily nuclear, but it is also enriched at the leading edge (indirect immunofluorescence, green) where it colocalizes with a subset of actin filaments (Alexa Fluor 568-phalloidin, red). Inset: leading edge, contrast enhanced to show actin filaments and JMY. Scale bar, 10 μ m.

(h) Models of *in vivo* role of JMY. Top, Model 1: JMY nucleates filaments that then serve as substrates for dendritic nucleation by Arp2/3. Bottom, Model 2: JMY evolved to nucleate actin in different cellular contexts. In the nucleus it

nucleates unbranched filaments, and in the cytoplasm it both nucleates filaments and activates Arp2/3.

Supplementary Figure S1. Expression of GFP-JMY in U2OS cells.

a, Expression of GFP-JMY (top panels), GFP-JMY Δ CA (center panels), and GFP-JMY Δ WWWCA (bottom panels) in U2OS cells. Cells were fixed and stained with Alexa Fluor 568 phalloidin (red) and DAPI (blue). All JMY constructs localize to cytoplasmic clusters (arrowheads) in addition to being diffuse in the cytoplasm. Ectopic filamentous actin structures colocalize with GFP-JMY and GFP-JMY Δ CA, but not GFP-JMY Δ WWWCA.

b, Expression of GFP in U2OS cells. (Compare to expression of GFP-PWWWCA in Fig. 1). Scale bars, 20 μ m.

Supplementary Figure S2. *Wa*, *Wb*, and *Wc* are *bona fide* WH2 domains.

a, 10 μ M actin was polymerized with increasing concentrations of GST-*W_a*, in KMEI (see Methods). GST-*W_a* concentrations are indicated (in μ M). Traces are normalized relative to 10 μ M actin alone so as to not mask the effect of sequestration. Inhibition of spontaneous polymerization is evidence that these WH2 domains bind monomeric actin. GST-*W_b* and GST-*W_c* also inhibit spontaneous polymerization (not shown).

b, Alignment of WH2 domains from Spire, JMY, WHAMM, Cordon Bleu, and WASp-family proteins (ClustalW). Conserved hydrophobic residues are highlighted gray, and conserved basic residues are highlighted red. JMY WH2

domains were identified by searching genome databases using a consensus WH2 domain sequence derived from a combination of sequence conservation, structural, and biochemical criteria.

Supplementary Figure S3. Biochemical characterization of JMY.

a-c, JMY does not affect elongation of preformed filaments. 4 μ M actin was polymerized alone or in the presence of preformed actin filament seeds, with or without 500 nM JMY WWCA (as noted). Polymerization rates were calculated during the linear phase of the reactions, between 40 and 180 s.

b, Cartoon depicting the three types of reactions occurring in the experiments. Experiments containing JMY and seeds represent a combination of all three reactions: (1) nucleation by JMY, (2) elongation off of pre-existing seeds, and (3) background spontaneous polymerization of actin.

c, Quantification of polymerization rates. Left: elongation rates for reactions. Right: stacked columns indicate that reactions containing seeds and JMY (left bar) are slower than the sum of JMY-nucleation plus seed elongation alone (right bar). This is consistent with the increased rate of polymerization in the presence of JMY being due to increased nucleation, not increased rate of elongation or filament severing. Spontaneous polymerization of actin also contributes to the observed rate of polymerization. To account for this reaction being represented twice in the bars on the right, we added this rate onto the left bar for reference (light gray, actin alone). Error bars, s.e.m.; n=4.

d-e, JMY WWCA does not cap the barbed ends of actin filaments. Capping protein slows depolymerization from the barbed end of actin filaments, whereas JMY does not. Increased rate of depolymerization at high concentrations of JMY (consistent with Spire results¹) is likely due to sequestration of actin monomers by JMY. Initial rate of depolymerization for reactions is plotted in **e**. Error bars, s.e.m.; n=3.

f-g, JMY WWCA does not cap the pointed ends of gelsolin-capped actin filaments. The Arp2/3 complex binds to the pointed end of actin filaments, and slows pointed end depolymerization, whereas JMY does not. Initial rate of depolymerization for reactions is plotted in **g**. Error bars, s.e.m.; n=3.

h-i, JMY fragments composed of the two C-terminal WH2 domains (W_b and W_c) nucleate actin, but maximal activity requires all three WH2 domains. Similarly, reactions with WWWCA and Arp2/3 (red) are faster than those with WWCA and Arp2/3 (green). **i**, Dose curves of nucleation and activation of the Arp2/3 complex by JMY WWWCA (as in Fig. 1f) and JMY WWCA.

j, Conserved tryptophan in the JMY acidic domain is important for activating the Arp2/3 complex, but not for JMY's intrinsic nucleation. This is consistent with JMY activating the Arp2/3 complex by the same mechanism as WASp-family proteins, and agrees with our results using WWW and W_bW_c , which indicate that only JMY WH2 domains contribute to nucleation. Experimental conditions as in Fig. 1c.

k-l, Nucleation by JMY and Spire displays similar kinetics over a range of actin concentrations. Pyrene-actin polymerization assays with 167 nM JMY W_bW_c or

Spire CD and increasing concentrations of actin. Reactions containing 8 μ M actin are shown in **a**. Time to half-maximal fluorescence ($t_{1/2}$) was calculated as in Fig. 1d.

m-n, Critical concentration experiments. Pyrene-actin was polymerized and diluted into KMEI, alone (red) or containing Latrunculin B (black), 60 nM capping protein (gray), or 5 μ M JMY (blue). Fluorescence was measured after 14-18 hours. **n**, Critical concentration plotted as a function of concentration of JMY WWCA (blue) or N-WASp WWCA (orange). Like Spire¹, JMY WWCA weakly sequesters actin monomers, and N-WASp sequesters even more weakly.

o-p, Dose-curves of loss of function (**o**) and gain of function (**p**) mutations presented in Fig. 3. Time to half-maximal fluorescence ($t_{1/2}$) is plotted, over a range of concentrations, for each construct.

Supplementary Figure S4. Localization of JMY

a, JMY is primarily nuclear in multiple cell types. MEFs were fixed and imaged by indirect immunofluorescence with anti-JMY antibody 1289 as in Fig. 4 (green in merged image). Filamentous actin was visualized with Alexa Fluor 568 phalloidin (red). DNA was visualized with DAPI (blue).

b, In ruffling B16-F10 mouse melanoma cells, cytoplasmic JMY localizes to the leading edge. Two examples are shown.

c, GFP-JMY expression in spreading U2OS cells. The majority of GFP-JMY is cytoplasmic, but a fraction colocalizes with actin filaments at the leading edge. The box highlights the region expanded in bottom panels. Scale bars, 10 μ m.

d, Full-length, his-tagged JMY does not copellet with actin filaments. Actin was polymerized in 1x KMEI and incubated with serial dilutions of JMY or buffer alone, then actin filaments were pelleted. Gel shows supernatants (left) and pellets (right) of actin alone, JMY alone, and 5 serial dilutions of JMY.

Supplementary Figure S5. JMY in HL-60 cells and human neutrophils

a, d, Examples of human neutrophils (**a**) and HL-60 cells (**d**) stimulated with fMLP, as in Fig. 4. Micrographs show merged epifluorescence image, phalloidin (red), endogenous JMY (green), and DAPI. Transillumination micrographs are shown for reference.

b, Western blot of JMY in high speed supernatants of cytosol from undifferentiated HL-60 cells (H) recognizes a single, major band with an apparent molecular weight of 110 kDa, consistent with the predicted molecular weight of JMY. The antibody recognizes purified JMY WWCA (J), but not N-WASp WWCA (N) or Scar WCA (S), demonstrating that it is specific for JMY.

c, HL-60 cells were differentiated with 1.3% DMSO. At various time points cells were removed from the differentiating population, stimulated with fMLP, and immediately fixed and stained as in Fig. 5. JMY localization was scored as either mostly nuclear, mostly cytoplasmic, or at the leading edge; and cell morphology was scored as nonpolar or polar, based on phalloidin staining of actin filaments. Cartoon on the right depicts the different classes of cells plotted in the graph. Note that JMY begins to leave the nucleus on the first day of differentiation, and cells begin to polarize in response to fMLP by the third day.

e-g, We fixed and stained differentiated, stimulated HL-60 cells that expressed GFP (kind gift of O. Weiner, UCSF) for endogenous JMY, using Alexa Fluor 647 anti-rabbit secondary (Invitrogen). **e** shows a representative cell with JMY colocalized with actin filaments at the leading edge, as in Fig 4c. **f** shows GFP and JMY in the same cell. **g**, intensity was measured along the line shown in **f**, from the closed circle to the open circle, and plotted as a function of position (NIH ImageJ). The ratio of JMY to GFP was overlaid (blue), demonstrating that JMY is enriched relative to GFP at the leading edge of the cell.

Supplementary Figure S6. JMY contributes to cell migration.

a, GFP-JMY expression in U2OS cells used in wound healing assays (Fig. 5). Cells were FACS sorted for purity, seeded at 900 thousand cells per well of a 12 well plate, grown overnight, then scratch-wounded with a pipette tip. Micrograph shows wounded cells in phase (left), epifluorescence (center), and merged (right). Scale bar, 100 μm .

b, U2OS cells expressing GFP-JMY Δ CA migrate at the same rate as wild-type cells. Phase contrast images of a representative wound healing assay quantified in Fig. 5. Scale bar, 100 μm .

c-d, Wound healing assays in HEK 293 cells indicate that knocking-down JMY by RNAi impairs cell migration. (Conditions as in Fig. 5; n=7).

e-f, Western blots show RNAi efficiency in HEK 293 cells, using pooled siRNAs as in Fig 5 (**e**, top panel), shRNA plasmid (**e**, bottom panel, serial dilutions of cell

lysate) or individual siRNAs (f). C, control non-targeting 2 (Dharmacon) siRNA. Mock, shRNA empty vector

g, Quantification of wound closure after 24 hours in HEK 293 cells treated with individual JMY siRNAs (JMY-1, JMY-2, JMY-3) or control siRNA. Knockdown of JMY expression with all three siRNAs cause a wound healing defect.

h-i, Mutating nonconserved cysteine 978 to serine has no effect on Arp2/3 activation by JMY WCA. h, Alignment of JMY acidic domains shows that cysteine 978 is poorly conserved in available sequences (ClustalW). i, Activation of the Arp2/3 complex by JMY WCA and WCA(C978S) display identical kinetics after a day-long purification. After this time, the activity of WCA decreases quickly, while the activity of WCA(C978S) is stable for several days-weeks. Experimental conditions as in Fig. 1c.

Supplementary Figure S7. An explanation for almost everything.

I, Algal bloom (*Phyteria*) kills fish. **II**, No fish to eat frog spawn, so an outbreak ensues. **III-IV**, Frogs die from poisoned water (I) and thus are unable to consume lice (III) and fly (IV) larvae, causing outbreak of each. **V**, Lice from III spread blue tongue to cattle and African horse sickness to horses. **VI**, Glanders, a WWI biowarfare agent, is carried by flies from IV. **VII**, Hail happens. **VIII**, So do locusts, periodically. **IX**, Sandstorm or volcanic eruption on Santorini, and then I see a darkness. **X**, *Stachybotrysatra* mold grows on the top of damp grain. Most important people (Egyptians) get served from the top, and first-born males get an extra portion, and are thus selectively poisoned. **XI**, Molecular biology is hard.

Figure 1

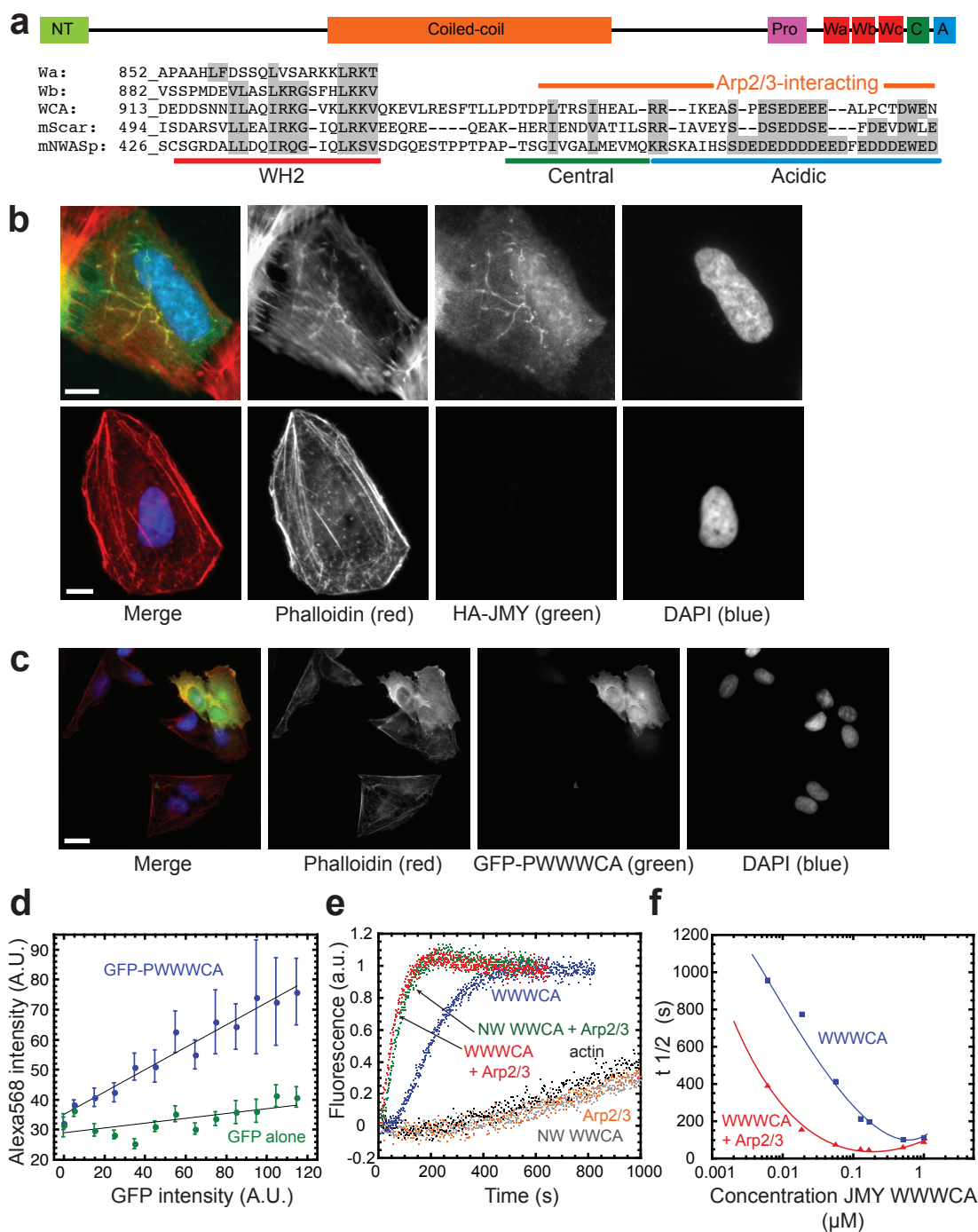


Figure 2

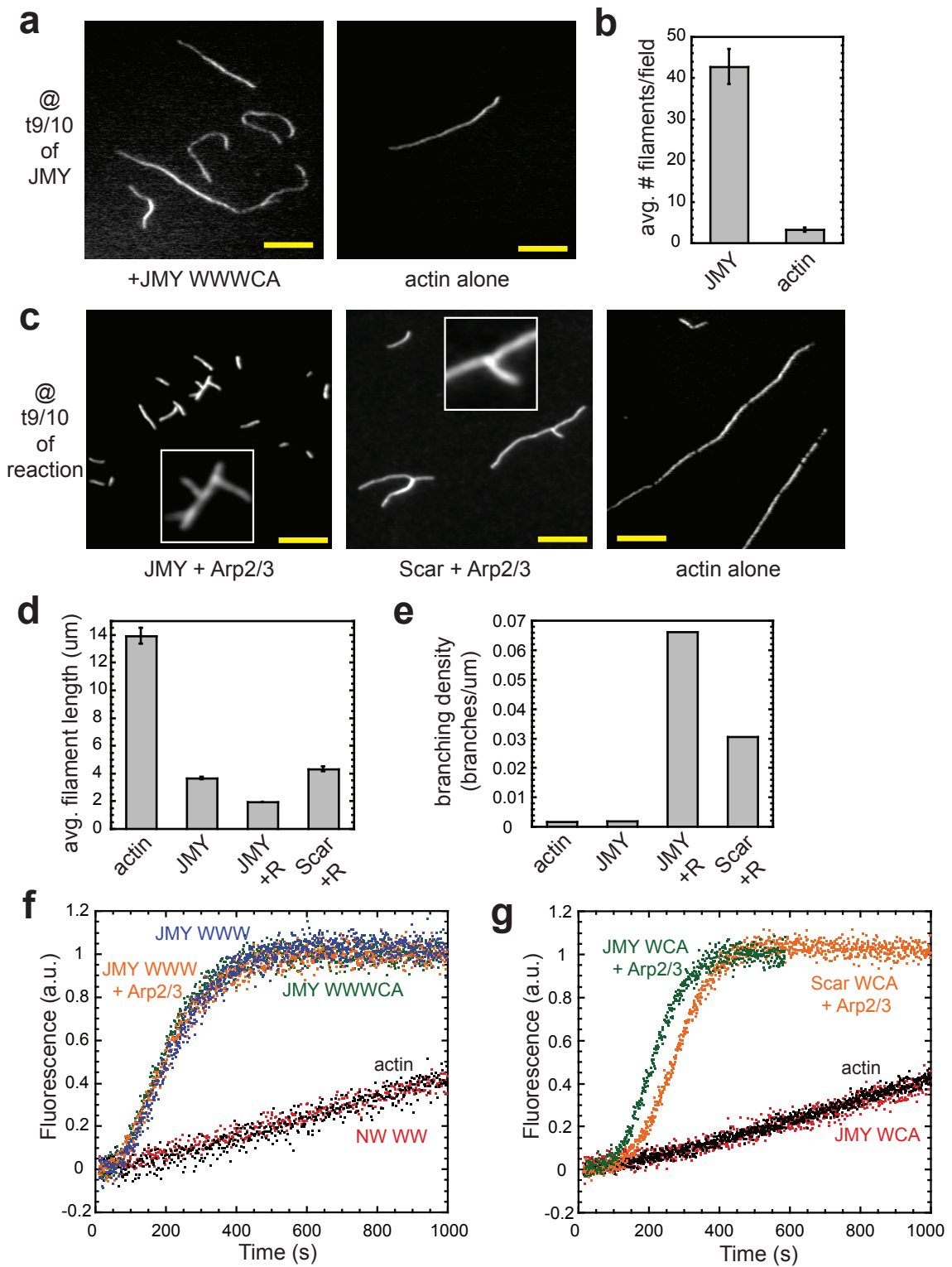


Figure 3

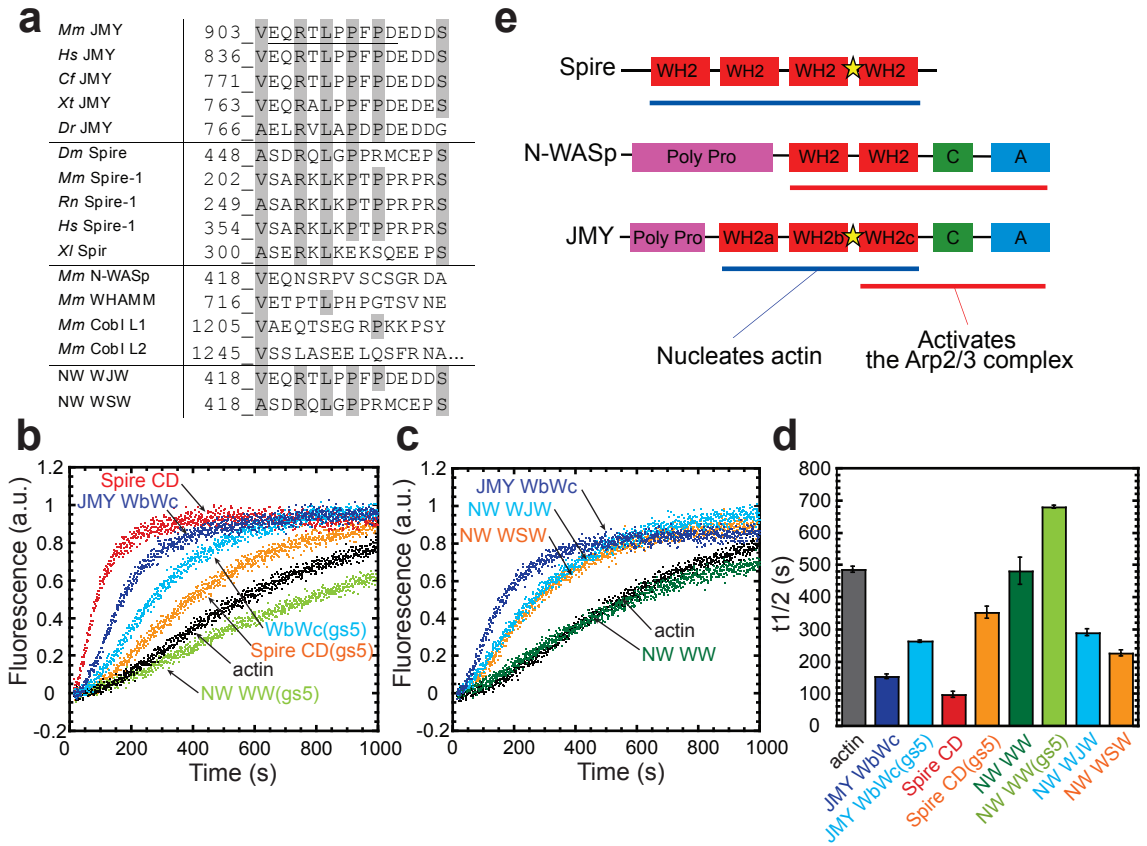


Figure 4

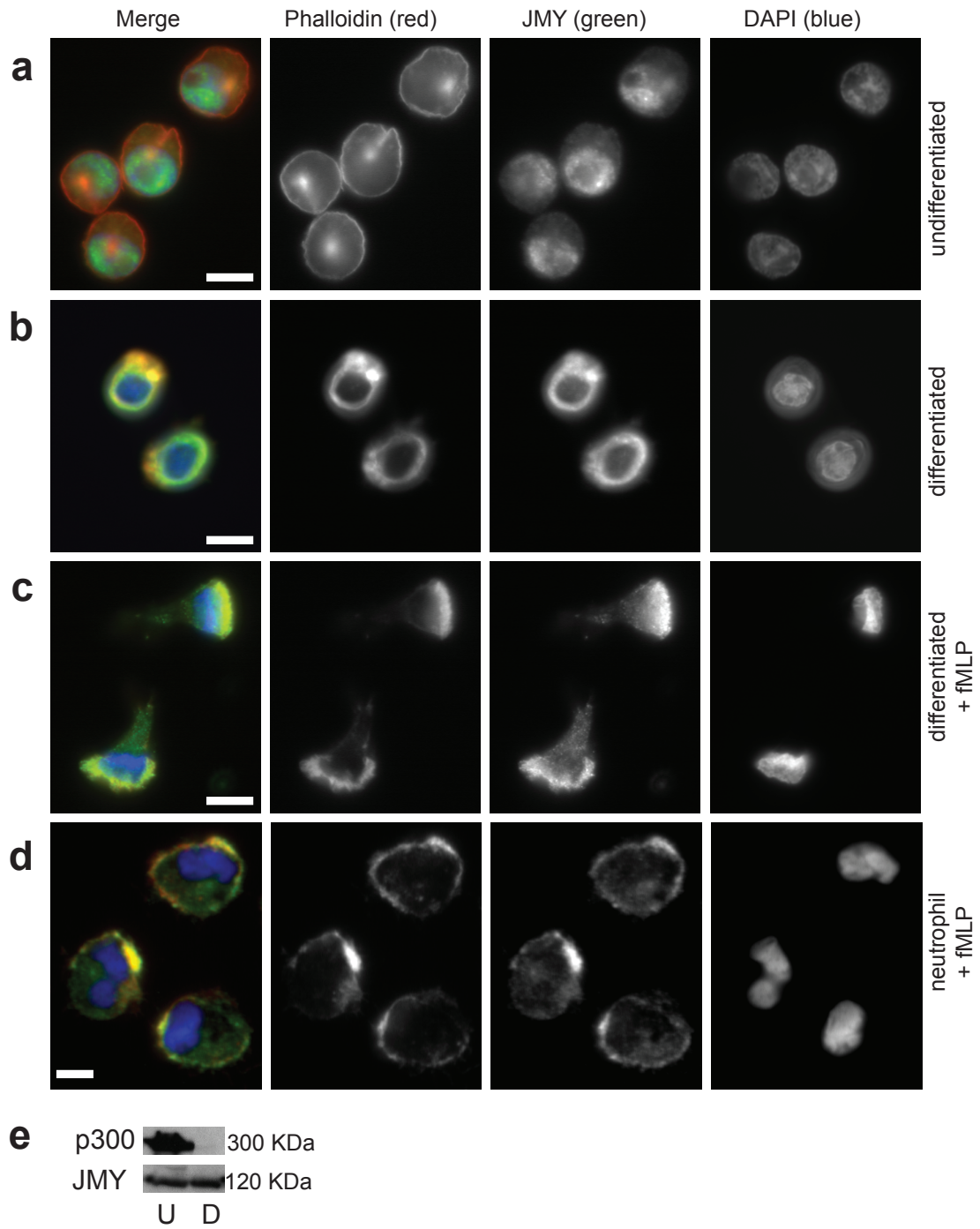
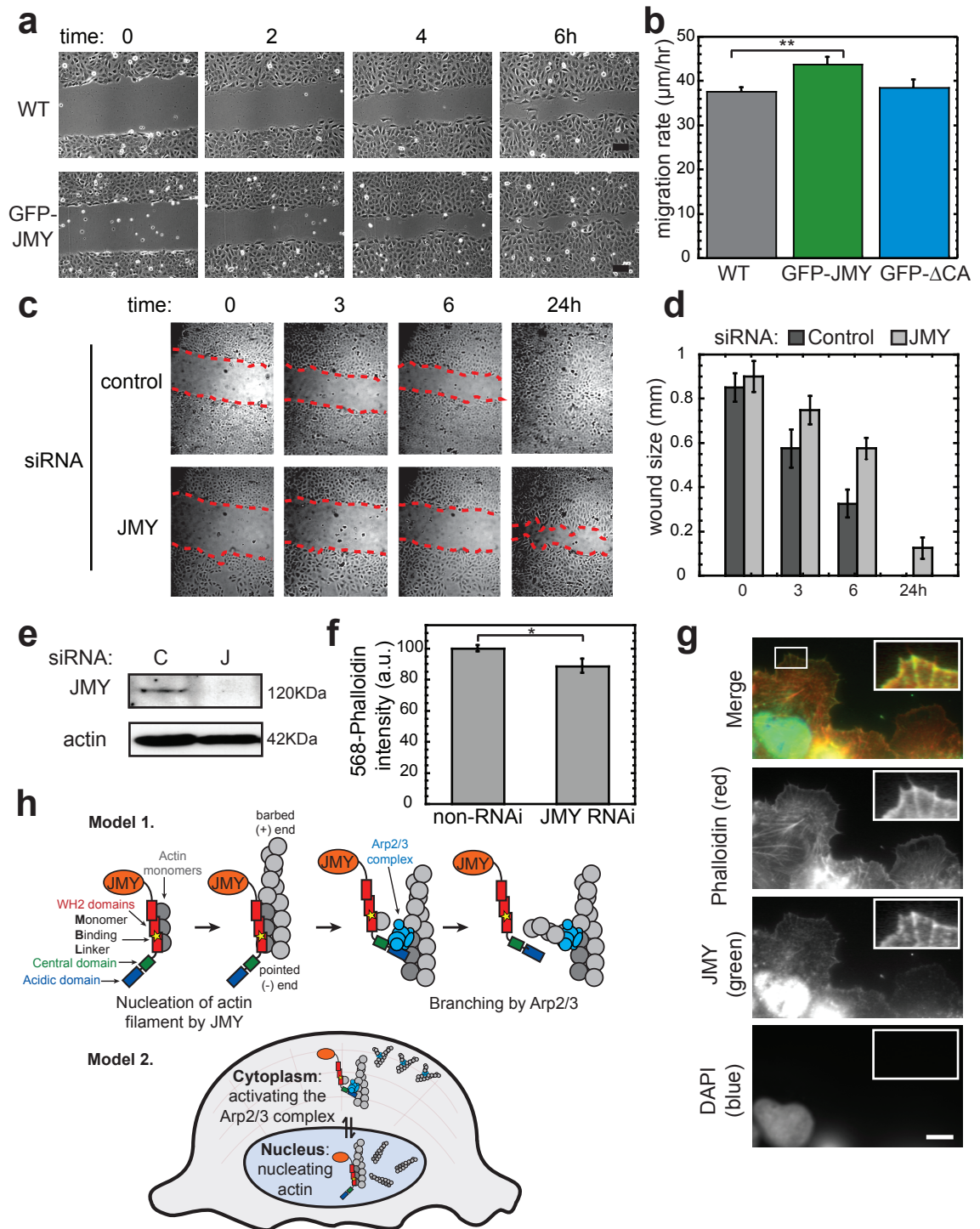
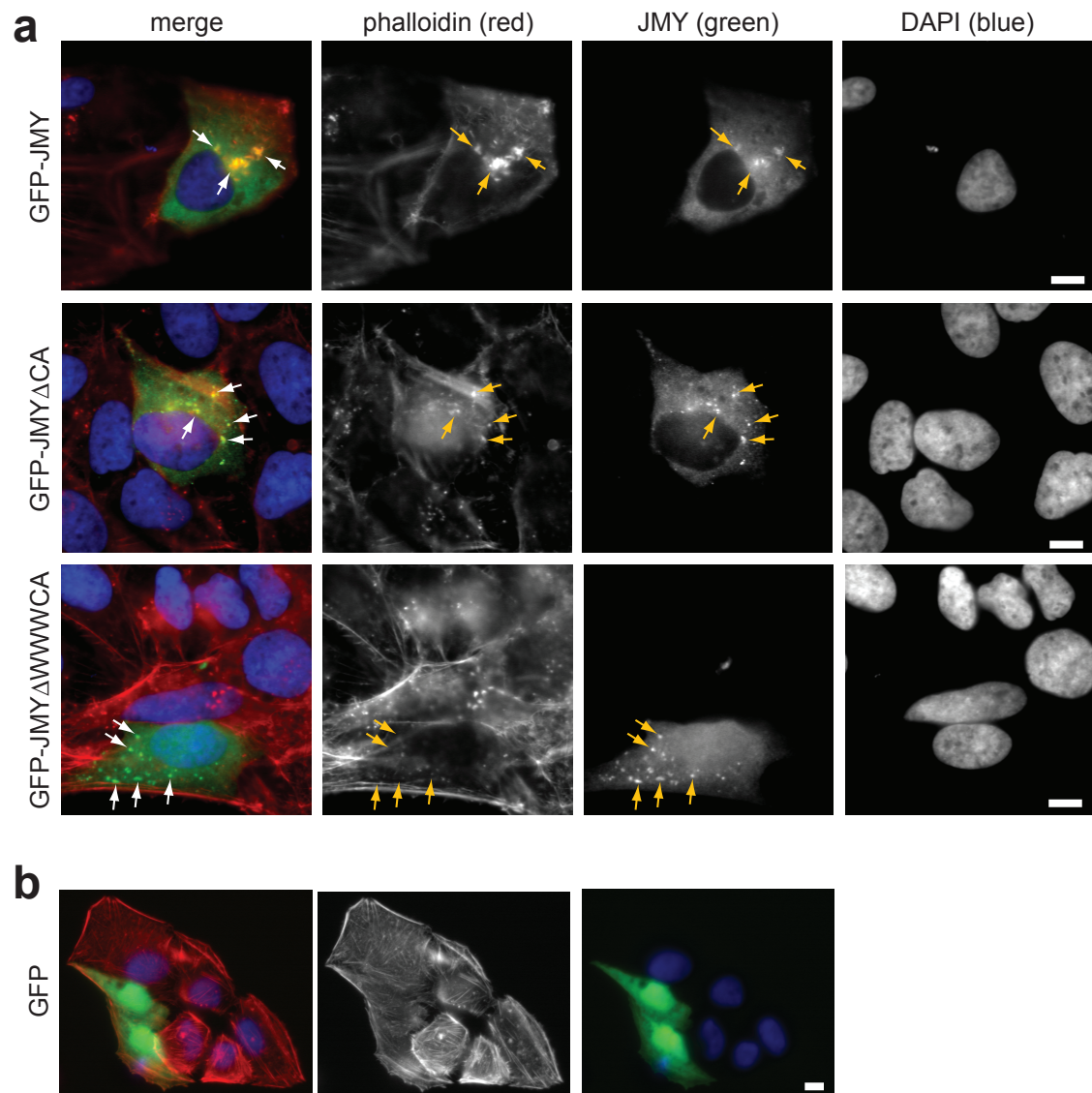


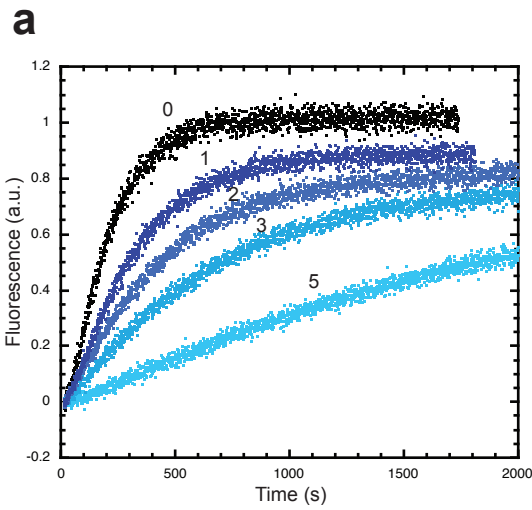
Figure 5



Supplementary Figure S1



Supplementary Figure S2

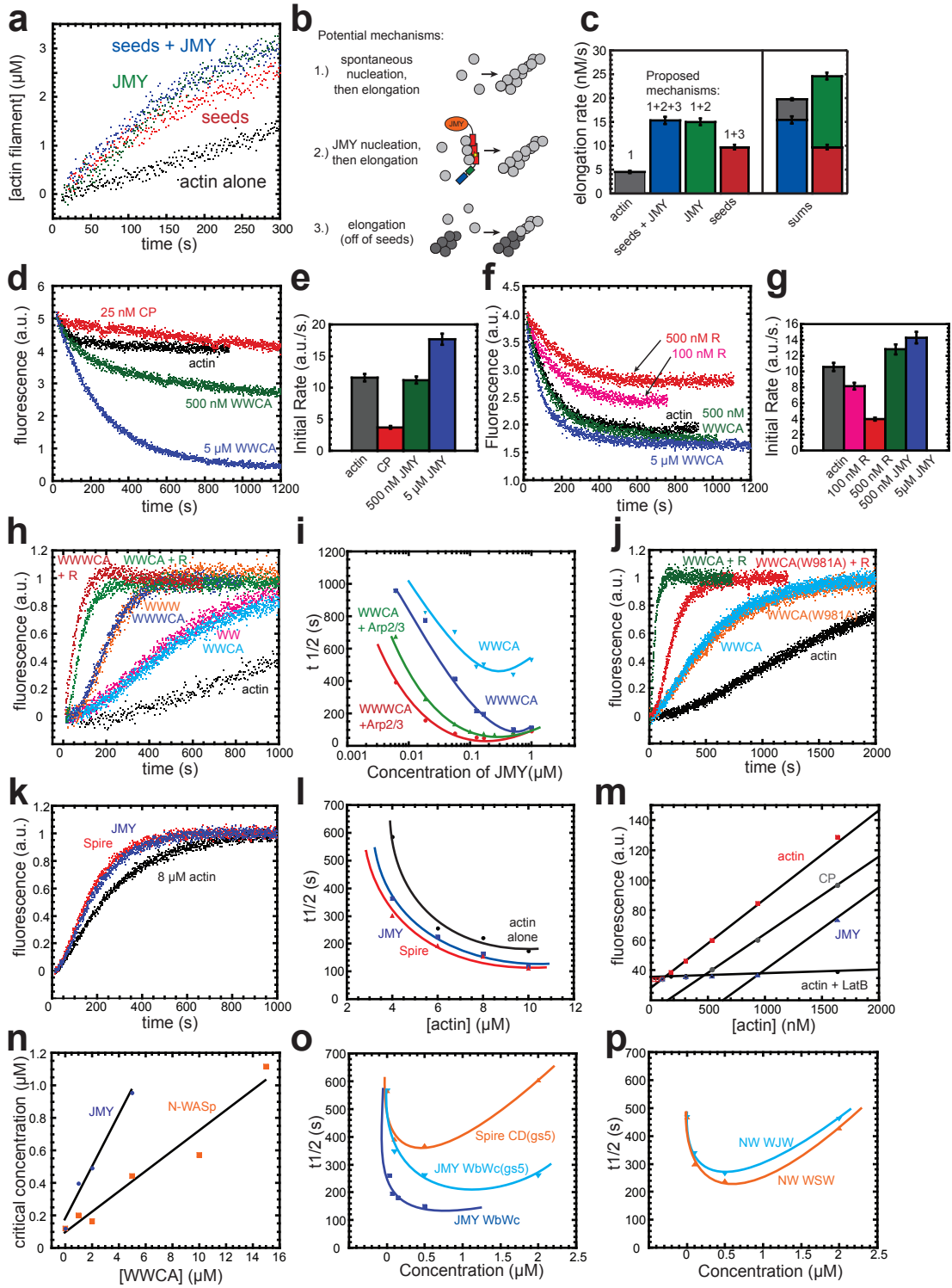


JMY Wa	<i>M. musculus</i>	AAHLFDSSQLVSAARKKLRKT
	<i>B. taurus</i>	SAHLFDSSQLVSAARKKLRKT
	<i>H. sapien</i>	SAHLFDSSQLVSAARKKLRKT
	<i>X. tropicalis</i>	LAQLFDSSQLLNARKTLKKT
	<i>D. rerio</i>	SARFFDSSQLLNARKKLRKT
	<i>T. nigroviridis</i>	SPRFFDSSQLQTARKKLRKT
	<i>C. familiaris</i>	SAHLFDSSQLVSAARKKLRKT
JMY Wb	<i>M. musculus</i>	SPMDEVLASLKRGSFHLKVV
	<i>R. norvegicus</i>	SPMDEVLASLKRGSFHLKVV
	<i>H. sapien</i>	SPMDEVLASLKRGSFHLKVV
	<i>X. tropicalis</i>	SPMDEVLASLKRGSFHLKVV
	<i>D. rerio</i>	SPMDEVLASLKRGSFHLRKA
	<i>P. troglodytes</i>	SPMDEVLASLKRGSFHLKVV
WHAMM W1	<i>M. musculus</i>	GSMDEVLASLRQ GKASLRKV
	<i>H. sapien</i>	GSMDEVLASLRHGRAPLRKV
JMY Wc	<i>M. musculus</i>	DDSNNILAQIRKGVK-LKKV
	<i>R. norvegicus</i>	DDSNNILAQIRKGVK-LKKV
	<i>H. sapien</i>	DDSNNILAQIRKGVK-LKKV
	<i>X. tropicalis</i>	DESNNILAQIRKGVK-LKKV
	<i>D. rerio</i>	DDGNNILAQIRKGVK-LRKV
	<i>P. troglodytes</i>	DDSNNILAQIRKGVK-LKKV
WHAMM W2	<i>M. musculus</i>	SNNEQLAAIRQGVQ-LKKV
	<i>H. sapien</i>	SNNEHLLAAIRQGVK-LKKV

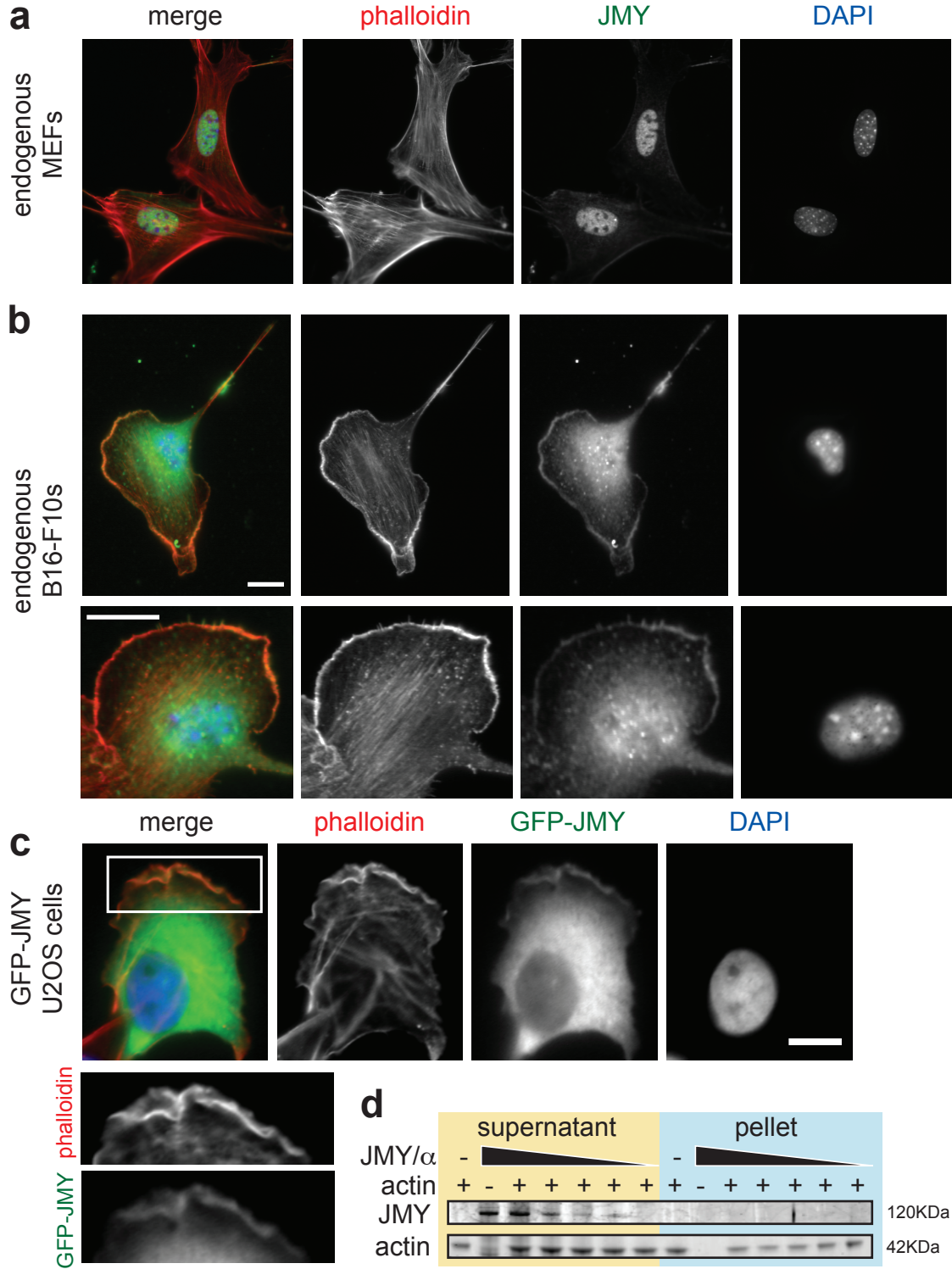
b

Spire A	<i>M. musculus</i> Spire-1	ARFWVQVMRDRLRNGVKLRKV
	<i>R. norvegicus</i> Spire-1	ARFWVQVMRDRLRNGVKLRKV
	<i>H. sapien</i> Spire-1	ARFWVQVMRDRLRNGVKLRKV
	<i>X. laevis</i> Spire	GNLWSNVIKELRLGIRLRNS
	<i>M. musculus</i> Spire-2	ARLWVQLMRELRRHGVLKRV
	<i>R. norvegicus</i> Spire-2	ARLWVQLMRELRRHGVLKRV
	<i>H. sapien</i> Spire-2	ARLWVQLMRELRRHGVLKRV
<i>D. melanoga ster</i> Spire	ARFWVQVIDELRRGVRLKKS	
Spire B	<i>M. musculus</i> Spire-1	TPYEMLMDDIRCKRYTLRKV
	<i>R. norvegicus</i> Spire-1	TPYEMLMDDIRCKRYTLRKV
	<i>H. sapien</i> Spire-1	TPYEMLMDDIRCKRYTLRKV
	<i>X. laevis</i> Spire	TPFELLMNDIRAKRYTLREV
	<i>M. musculus</i> Spire-2	TPFEMLMQDIRARNYKLRKV
	<i>R. norvegicus</i> Spire-2	TPFEMLMQDIRARNYKLRKV
	<i>H. sapien</i> Spire-2	TPFEMLMQDIRARNYKLRKV
<i>D. melanoga ster</i> Spire	TPYEILMGDIRAKRYQLRKV	
Spire C	<i>M. musculus</i> Spire-1	KSAHEVILDFIRSRPPLNRPV
	<i>R. norvegicus</i> Spire-1	KSAHEVILDFIRSRPPLNPA
	<i>H. sapien</i> Spire-1	KSAHEVILDFIRSRPPLNRPV
	<i>X. laevis</i> Spire	QSVENFIMDFIRSQP-LRPA
	<i>M. musculus</i> Spire-2	KDAHEVILDFIRSRPPLKQV
	<i>R. norvegicus</i> Spire-2	KDAHEVILDFIRSRPPLKQV
	<i>H. sapien</i> Spire-2	KDAHEVILDFIRSRPPLKQV
<i>D. melanoga ster</i> Spire	KDAHAMILEFIRSRPPLKKA	
Spire D	<i>M. musculus</i> Spire-1	SLHERILEEIKAEER-LRPV
	<i>R. norvegicus</i> Spire-1	SLHERILEEIKAEER-LRPV
	<i>H. sapien</i> Spire-1	SLHERILEEIKAEER-LRPV
	<i>X. laevis</i> Spire	SLHELLMSEIKSGKK-LRST
	<i>M. musculus</i> Spire-2	TLHEKILEEIKQERR-LRPV
	<i>R. norvegicus</i> Spire-2	TLHEKILEEIKQERR-LRPV
	<i>H. sapien</i> Spire-2	SLHEKILEEIKQERR-LRPV
<i>D. melanoga ster</i> Spire	SPREQLMESIRKGE-LKQI	
Others	<i>H. sapien</i> N-WAS p Wa	GNKAALLDQIREGAQ-LKKV
	<i>M. musculus</i> N-WAS p Wa	GNKAALLDQIREGAQ-LKKV
	<i>H. sapien</i> N-WAS p Wb	SGRDALLDQIRQGIQ-LKS V
	<i>M. musculus</i> N-WASp Wb	SGRDALLDQIRQGIQ-LKS V
	<i>H. sapien</i> Scar-1	DARSVLLAARIRKGIQ-LRKV
	<i>H. sapien</i> Scar-3	DARSDLLAARIRMGIQ-LKKV
	<i>D. melanoga ster</i> Scar	DPNRNDLMKAIIRDGIT-LRKV
<i>M. musculus</i> Cobl W1	HSALMEAIHSGGRE-LRKV	
<i>M. musculus</i> Cobl W2	RSALLAAIRGHSGTSLRKV	
<i>M. musculus</i> Cobl W3	RQALMDAIRSGTGAA-LRKV	

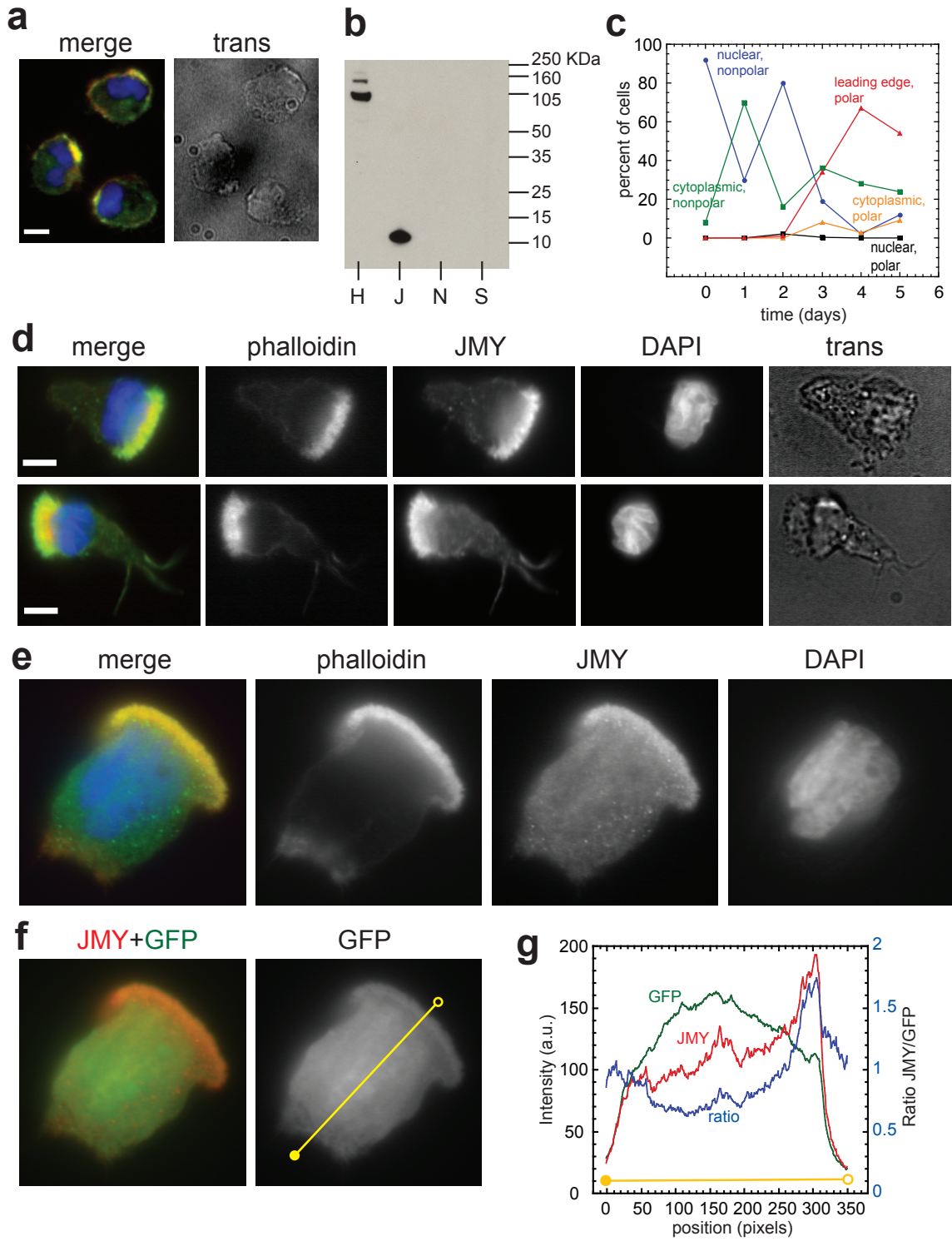
Supplementary Figure S3



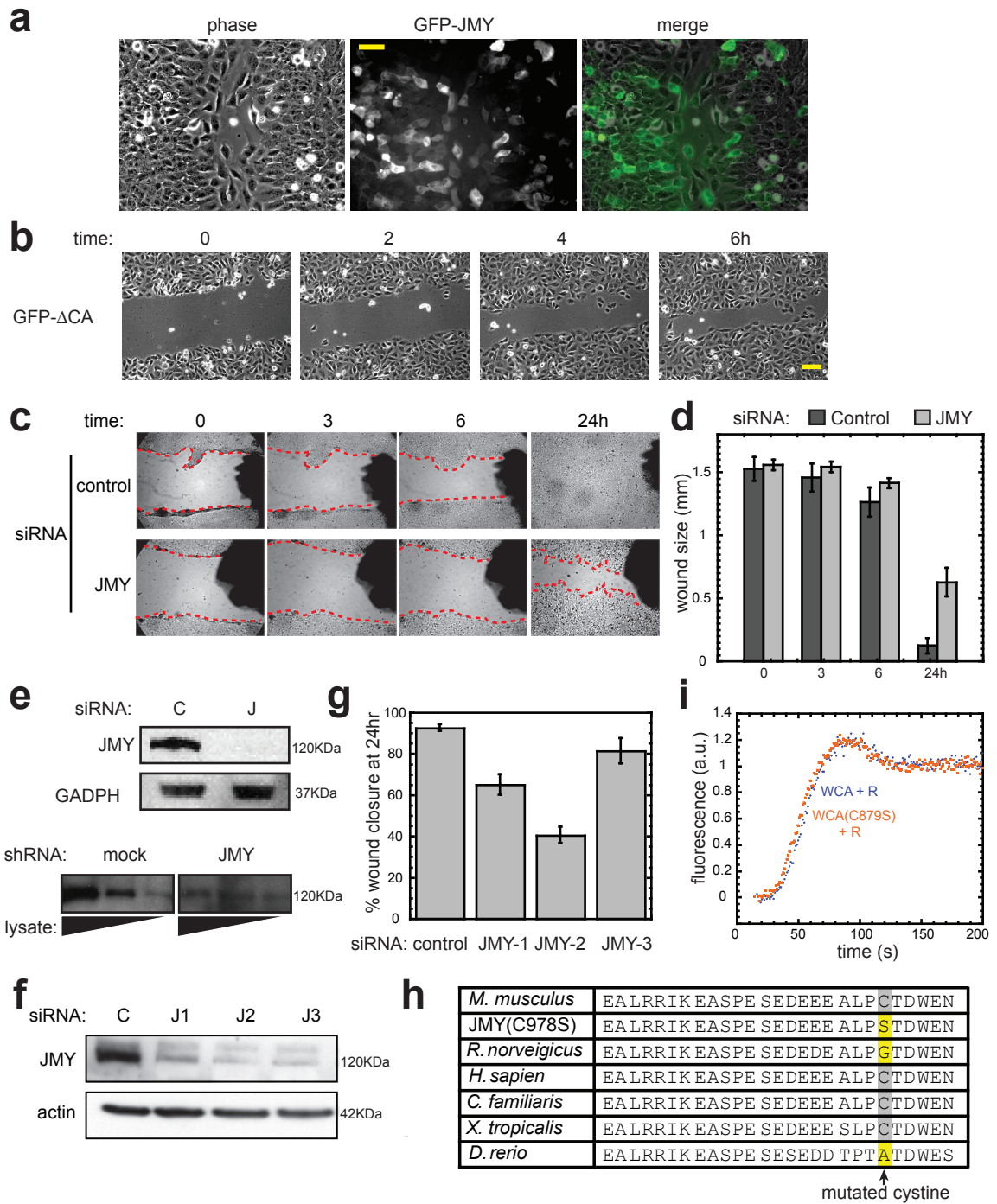
Supplemental Figure S4



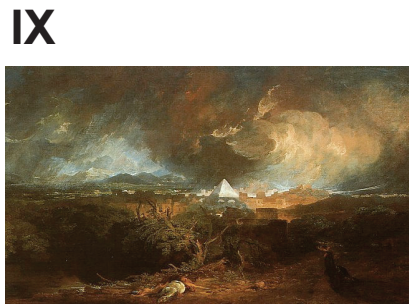
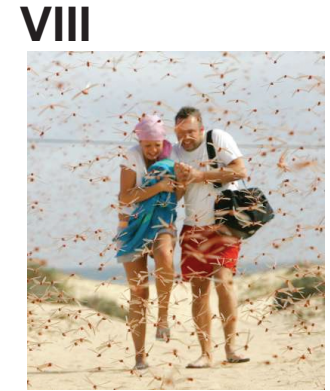
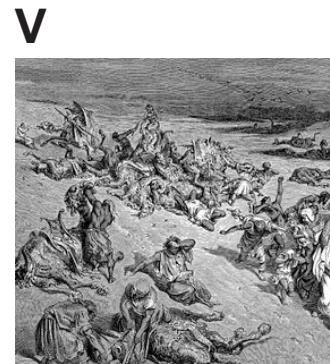
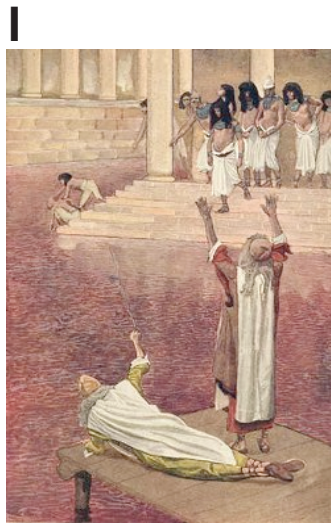
Supplementary Figure S5



Supplementary Figure S6



Supplementary Figure S7

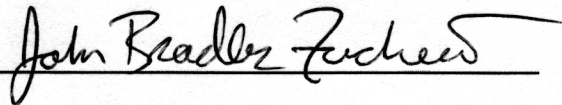


Publishing Agreement

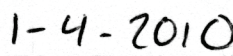
It is the policy of the University to encourage the distribution of all theses, dissertations, and manuscripts. Copies of all UCSF theses, dissertations, and manuscripts will be routed to the library via the Graduate Division. The library will make all theses, dissertations, and manuscripts accessible to the public and will preserve these to the best of their abilities, in perpetuity.

Please sign the following statement:

I hereby grant permission to the Graduate Division of the University of California, San Francisco to release copies of my thesis, dissertation, or manuscript to the Campus Library to provide access and preservation, in whole or in part, in perpetuity.



Author signature



date